Published in final edited form as:
Biochim Biophys Acta. 2014 December ; 1843(12): 2855–2870. doi:10.1016/j.bbamcr.2014.08.008.

Human erythrocyte Band 3 functions as a receptor for the sialic acid-independent invasion of *Plasmodium falciparum*. Role of the RhopH3-MSP1 complex

Michael Baldwin[‡,*], **Innocent Yamodo**[§,*], **Ravi Ranjan**[¶], **Xuerong Li**[¶], **Gregory Mines**[‡], **Marina Marinkovic**[‡], **Toshihiko Hanada**[‡], **Steven S. Oh**[§], and **Athar H. Chishti**[‡]

[‡]Department of Developmental, Molecular & Chemical Biology, Tufts University School of Medicine and Program in Cellular and Molecular Physiology, Sackler School of Graduate Biomedical Sciences, Boston, MA 02111

[¶]Department of Pharmacology, University of Illinois College of Medicine, Chicago, Illinois 60612

[§]St. Elizabeth's Medical Center, Tufts University School of Medicine, Boston, Massachusetts 02135

Abstract

Plasmodium falciparum takes advantage of two broadly defined alternate invasion pathways when infecting human erythrocytes: one that depends on and the other that is independent of host sialic acid residues on the erythrocyte surface. Within the sialic acid-dependent (SAD) and sialic acid-independent (SAID) invasion pathways, several alternate host receptors are used by *Plasmodium falciparum* based on its particular invasion phenotype. Earlier, we reported that two putative extracellular regions of human erythrocyte band 3 termed 5C and 6A function as host invasion receptor segments binding parasite proteins MSP1 and MSP9 via a SAID mechanism. In this study, we developed two mono-specific anti-peptide chicken IgY antibodies to demonstrate that the 5C and 6A regions of band 3 are exposed on the surface of human erythrocytes. These antibodies inhibited erythrocyte invasion by the *Plasmodium falciparum* 3D7 and 7G8 strains (SAID invasion phenotype), and the blocking effect was enhanced in sialic acid-depleted erythrocytes. In contrast, the IgY antibodies had only a marginal inhibitory effect on FCR3 and Dd2 strains (SAD invasion phenotype). A direct biochemical interaction between erythrocyte band 3 epitopes and parasite RhopH3, identified by the yeast two-hybrid screen, was established. RhopH3 formed a complex with $MSP1_{19}$ and 5ABC region of band 3, and a recombinant segment of RhopH3 inhibited parasite invasion in human erythrocytes. Together, these findings provide evidence that erythrocyte band 3 functions as a major host invasion receptor in the SAID invasion pathway by assembling a multi-protein complex composed of parasite ligands RhopH3 and MSP1.

Corresponding author. Athar Chishti, Department of Developmental, Molecular & Chemical Biology, Tufts University School of Medicine, 150 Harrison Avenue, Room 714, Boston, MA. 02111, Tel: (617) 636-3457; Fax: (617) 636-3568; athar.chishti@tufts.edu.
*Both authors contributed equally to this work.

Keywords

Plasmodium falciparum; Erythrocyte; Band 3; Chicken antibodies; RhopH3; MSP1

1. Introduction

Red blood cell (RBC) invasion by malaria parasites involves complex yet precisely timed events that require specific host-parasite interactions [1, 2]. In *Plasmodium falciparum*, two unique RBC invasion phenotypes have been observed in the field [3–5] and laboratory culture [6–9]: one that largely relies on sialic acid residues of RBC sialoglycoproteins for invasion (e.g., FCR3, Dd2, W2-mef, Camp, and FVO strains) and the other which does not depend on RBC sialic acids (e.g., 3D7, 7G8, FCB-1, HB3, and Thai-2 strains). These observations led to the recognition of two distinct RBC invasion pathways involving either a sialic acid-dependent (SAD) or sialic acid-independent (SAID) mechanism. In the SAD invasion pathway, RBC sialoglycoproteins such as glycophorins are known to serve as major invasion receptors interacting with parasite ligands EBA-175 [10–14], EBL-1 [15, 16], and EBA-140 (also known as BAEBL) [17–20]. In addition, several hypothetical RBC sialoglycoproteins have been implicated as host invasion receptors associating with *P. falciparum* proteins such as Rh1 and EBA-181 (also known as JESEBL) by a SAD mechanism [14, 21]. However, it is known that RBCs lacking glycophorins are invaded, albeit at a reduced rate, by the field isolates of *P. falciparum* indicating the existence of SAID invasion pathways.

In the SAID invasion pathway, the hypothetical RBC receptor X interacting with an unidentified *P. falciparum* merozoite protein [22, 23] and the hypothetical receptor Z interacting with *P. falciparum* Rh2b [24] have been proposed. RBC antigen Kx, modified by a trypsin-like enzyme, is known to interact with *P. falciparum* AMA-1 during invasion by a SAID mechanism [25]. Similarly, the complement receptor 1 (CR1) has been identified as a host receptor for the SAID invasion pathway interacting with *P. falciparum* Rh4 [26, 27]. Recently, erythrocyte membrane protein Basigin has been identified as a host receptor interacting with *P. falciparum* Rh5 [28]. Earlier, we reported that two putative exofacial regions of human RBC band 3 termed 5ABC (amino acids 720-761) and 6A (amino acids 807-826) function as a non-glycosylated invasion receptor binding to the 19 kDa and/or 42 kDa C-terminal processing product(s) of *P. falciparum* MSP1 (termed $MSP1_{19}$ and $MSP1_{42}$, respectively), a major GPI-anchored merozoite surface protein [29]. The invasion receptor activity was most noteworthy at the 5C (amino acids 742-761, the C-terminal half of 5ABC) and 6A regions based on the invasion blocking assay using the *P. falciparum* 3D7 strain [29]. Our subsequent studies have shown that two regions of *P. falciparum* MSP9 (also known as ABRA and p101) also interact directly with the 5ABC region of band 3 [30], while forming a co-ligand complex with $MSP1_{19}$ (or $MSP1_{42}$) [31]. Specific complex formation between MSP1 and MSP9 was further supported by subsequent mapping of a *P. falciparum* protein interaction network in which the MSP1-MSP9 interaction was central to a large cluster of invasion-related protein interaction network [32].

Human RBC band 3 consisting of 911 amino acids is characterized by an N-terminal cytoplasmic domain, C-terminal membrane-embedded domain, and C-terminal cytoplasmic

tail [33, 34]. The N-terminal cytoplasmic domain provides an anchoring site for the RBC skeleton, deoxyhemoglobin, glycolytic enzymes, and the protein tyrosine kinase p72syk [35–37]. The C-terminal membrane-spanning domain catalyzes the exchange of anions (Cl^- for $HCO3^-$) across the membrane to increase the CO_2 transport capacity in RBCs [38]. The relatively short C-terminal cytoplasmic tail associates with carbonic anhydrase II required for moving CO_2 from tissues to the lung [39]. A high-resolution crystal structure of the N-terminal cytoplasmic domain has been reported [36], whereas several low-resolution three-dimensional maps of the membrane-spanning domain of band 3 are also available [40]. Computer generated topology models of human RBC band 3 predict the protein spans the lipid bilayer 12–14 times giving rise to 6–7 extracellular domains [41]. The topology of transmembrane (TM) segments TM1 to TM9 (ending at Leu-724) is relatively well defined; however, the folding of the remaining TM segments starting with TM10 remains controversial. Three independent topology models predict a significant part of the 5C region is exposed on the RBC surface [42–44], and two of these models suggest a considerable part of the 6A region is also exposed [43, 44]. Recent determination of the structure of Band 3/AE1 membrane domain dimer at 7.5-Å resolution by electron microscopy revealed a partial exposure of the 5ABC region, particularly sequence corresponding to the 5C region, and somewhat ambiguous topology of the 6A region [45, 46]. Despite these structural insights, conclusive biochemical validation of the accessibility of specific regions of band 3 in intact erythrocytes is lacking.

In this study, we developed two anti-band 3 antibodies in chicken egg yolk using peptides patterned on the 5C and 6A regions of human RBC band 3. Using these IgY antibodies, we provide conclusive evidence that the two core regions of the band 3 invasion receptor, termed 5C and 6A are indeed exposed on the normal human RBC surface. These anti-5C and anti-6A antibodies inhibit RBC invasion by the 3D7 and 7G8 strains of *P. falciparum* (SAID invasion phenotype) at a significant rate when added to the parasite culture medium. On the other hand, these antibodies had little effect on blocking RBC invasion by the FCR3 and Dd2 strains (SAD invasion phenotype). We screened a yeast two-hybrid *P. falciparum* cDNA library using the 5ABC fragment of human band 3 as bait, and identified parasite RhopH3 as an interaction partner. We demonstrate the existence of a ternary complex between RhopH3, MSP1 and Band 3, and show that a putative extracellular domain of RhopH3 inhibits parasite invasion in human RBCs. Taken together, our results provide biochemical evidence that the 5C and 6A regions of human band 3 forming the erythrocyte invasion receptor are exposed on the host cell surface. These findings suggest that *P. falciparum* assembles a multi-protein complex containing RhopH3 and MSP1 on RBC band 3 to facilitate entry via a SAID invasion pathway.

2. Materials and methods

2.1. Parasites

The 3D7A (MRA-151), 7G8 (MRA-152), FCR3 (MRA-158), and Dd2 (MRA-156) strains of *P. falciparum* were obtained from Malaria Research and Reference Reagent Resource Center (Manassas, Virginia). The 3D7 strain described here refers to the 3D7A strain (MRA-151). Parasites were maintained in culture as described [31]. Briefly, parasites were

cultured in complete RPMI 1640 medium containing 0.5% w/v Albumax II in a 5% CO_2/1% O_2/balance N_2 gas mixture. The synchronization of parasites at the ring stage using 5% sorbitol, and enrichment of late-stage trophozoites using 63% (v/v) Percoll were carried out as described [29].

2.2. Anti-band 3 IgY and anti-RhopH3 antibodies

Peptides ASTPGAAAQIQEVKE and FKPPKYHPDVPYVK derived from the 5C and 6A regions of human erythrocyte band 3 (Fig. 1A) were each conjugated to Keyhole Limpet Hemocyanin (KLH) by an N-terminal cysteine coupling. Using these peptides, antibodies were produced in chickens by Sigma-Genosys. Following six injections given every 14 days, eggs were collected and antibody titer was determined by ELISA throughout the course of injections using blood serum. Total IgY antibodies were purified from the egg yolk using Eggcellent Chicken IgY Purification Kit (Pierce). Anti-5C and anti-6A IgY antibodies were affinity purified from corresponding total IgY using columns prepared by conjugating the above antigen peptides to the CNBr-activated resin (Pharmacia Biotech/GE Healthcare). The two mono-specific IgY antibodies were stored in PBS at 4°C. Eggs from two preimmune chickens were used to obtain total preimmune IgY antibodies as above. Peptide RDSSSDRILLEESKTFT derived carboxyl region of *P. falciparum* RhopH3 was conjugated to KLH by an N-terminal cysteine coupling. Antibodies against this peptide were raised in rabbit, and antibody titer and purification was performed as mentioned above. A preimmune serum from rabbit was used as control.

2.3. Recombinant proteins, RBC ghosts, enzymatic treatment of RBCs, and Western blotting

Total RNA was isolated from mixed stage culture of 8–10% parasitemia. Infected RBCs were lysed with 0.15% Saponin (1.5 vol) and parasite pellet was washed with PBS. Total RNA was isolated using TRIZOL Reagent following manufacturer's protocol (Invitrogen). The C-terminal fragment of RhopH3 (1858 – 2691 base pairs) was amplified from total RNA using the OneStep RT-PCR Kit (Qiagen) using the primers 5′-CGGGATCCTGTTTCTATCCAAAAGAATTTG-3′ and 5′-GCGTCGACCAATTC ATTTTCAGAAGTAAAGGTTTTAG-3′. The amplified product was cloned in pET32a expression vector (Novagen) to express fusion protein containing Thioredoxin (Trx) and Hexa-Histidine (His) tags at the N-terminus and a His tag at the C-terminus. Expression of GST-5ABC using the pGEX-2TK vector was described previously [29]. GST-6A was expressed by cloning the 6A region (amino acids 807-826) of the human erythrocyte band 3 gene into the same pGEX-2TK vector as described [29]. Recombinant MBP-$MSP1_{19}$ and Trx-$MSP1_{19}$ were purified as described previously [29]. The neuraminidase (Neu), Chymotrypsin (C), and Trypsin (T) treatment of intact RBCs to remove/deplete sialic acid residues from the RBC surface, and the preparation of human RBC ghosts were performed as described [29]. Removal of sialic acid residues on the RBC membrane was verified using GlycoProfile III Fluorescent Glycoprotein Detection Kit (Sigma), which is based on a modified Periodic Acid-Schiff method. Briefly, ghosts prepared from Neu-treated RBCs were subjected to SDS-PAGE, and the gel containing separated RBC proteins was treated with the Glyco-Pro reagents following the manufacturer's protocol. Carbohydrate-containing proteins were visualized as fluorescent bands directly on the gel using UV light.

Western blotting was carried out as described [31]. The mAb (clone BIII-136, mouse ascites fluid) against the N-terminal cytoplasmic domain of human RBC band 3 (anti-B3/cd mAb) was from Sigma. RBC binding experiments were performed as described previously [16, 47]. Briefly, 100 pmol of soluble Trx-RhopH3-C protein was incubated with 50 μl (packed cell volume) of normal and the enzyme treated RBCs containing 1% fetal bovine serum at 37°C for 2 h with gentle rocking, respectively. The mixture was layered over dibutyl phthalate, centrifuged, and supernatant was discarded. Bound protein was eluted with 15 μl of 1.5 M NaCl and analyzed by Western blotting using anti-His polyclonal antibody (GenScript). The Trx tag was used as a negative control.

2.4. Protein binding assays

For *in vitro* binding assays, different combinations of 50 pmol each of Trx-RhopH3-C, Trx-$MSP1_{19}$, and GST-5ABC were added in a reaction volume (200 μl) of binding buffer (50 mM Tris-HCl, pH 7.6, 1.0 mM EDTA, 5.0 mM $MgCl_2$, 0.1% NP40, 5.0 mM DTT, 1.0 mg/ml BSA and 150 mM NaCl) for 1.0 h at room temperature or overnight at 4°C. Bead-bound proteins were eluted and analyzed by Western blotting using respective antibodies [29]. Parasite supernatant binding was performed by adding 1 mL of culture supernatant to GST-5ABC protein immobilized on glutathione beads. Following binding for 2 hours at RT, beads were washed twice in RPMI, then eluted in SDS-sample buffer and analyzed by immunoblotting against RhopH3. Empty vector encoding GST was used as a negative control.

2.5. Immunofluorescence microscopy

Thin smears of normal and Neu-treated RBCs were fixed on glass slides with cold methanol for 30 min, blocked with 1% BSA in PBS (pH 7.4) for 30 min at RT, washed twice in PBS (5 min each), and incubated with affinity-purified anti-5C IgY or anti-6A IgY antibodies (100 μg/ml in 1% BSA in PBS). Preimmune IgY (100 μg/ml), the anti-B3/cd mAb, and the anti-GPA mAb reactive to extracellular residues of human GPA (Sigma) were also used as control. Slides were washed twice with PBS, incubated with appropriate secondary antibodies conjugated with Alexa 488 conjugate (green fluorescence) or Alexa 594 (red fluorescence) according to manufacturer's protocol (Invitrogen), and visualized at 100X magnification. Negative control included incubation of slides with the Alexa 488-conjugated anti-chicken secondary antibody alone.

2.6. Yeast two-hybrid library screen

The *P. falciparum* 3D7 cDNA library was constructed using HybriZap kit (Stratagene) from a pool of asynchronous parasite culture as described previously [29]. The bait construct pGBKT7-5ABC of human band 3 was transformed into yeast Y187 (Clontech) lacking autonomous transcriptional activation of the reporter gene [29]. The library screening was performed as described previously [30].

2.7. Quantitative ELISA

Quantification of recombinant RhopH3-C to band 3 (5ABC) and $MSP1_{19}$ was performed as described previously [30]. Briefly, ELISA plate was coated with GST and GST-5ABC in

carbonate buffer, pH 9.6, at 4°C overnight. After washing and blocking with PBS and PBST (0.1% Tween 20) containing 5% milk, the Trx and Trx-RhopH3-C proteins were added (0–5 μM). Upon incubation, bound protein was measured using anti-His polyclonal antibody (GenScript), anti-rabbit–HRP conjugated antibody, and TMB substrate (Pierce). Similarly, Trx and Trx-RhopH3-C were coated on the ELISA plate and MBP and MBP-MSP1$_{19}$ were added to the wells in varying concentrations (0–6 μM). Bound protein was measured using an anti-MBP antibody (NE BioLabs). Binding data were analyzed using SigmaPlot 11 (simple ligand binding using the equation for one site saturation).

2.8. Detection of antibody binding to RBCs by flow cytometry

Normal and Neu-treated intact human RBCs were washed with PBS and resuspended in RPMI (50% hematocrit). A 100 μl sample of the RBC suspension was incubated with anti-5C IgY (100 μg/ml), anti-6A IgY (100 μg/ml), preimmune IgY (100 μg/ml), anti-B3/cd mAb, or anti-GPA mAb for 30 min at 4°C. After three washes with PBS, the RBCs were resuspended in PBS containing FITC-conjugated anti-chicken or anti-mouse secondary antibody for 45 min at 4°C. Following three washes with PBS, the cells were resuspended in 300 μl of PBS and analyzed by recording 10,000 events using FACSCalibur (Becton Dickenson) equipped with a 15 mW Argon ion laser tuned at 488 nm. Fluorescent cell analysis was performed on the population gated on their forward scatter properties using the CellQuest (BD Bioscience) and WinMDI 2.8 software (http://facs.scripps.edu/software.html). Similarly, concentration-dependent binding of IgY antibodies to RBCs were carried out as described above. Briefly, normal and Neu-treated human RBCs were each incubated with a varying concentration (0, 25, 50, 100, 250 μg/ml) of anti-5C IgY, anti-6A IgY, or preimmune IgY in PBS. Mean fluorescence intensity (mean ± s.e.) from triplicate assays was plot against the IgY concentration. Student's *t*-test was used to compare the mean. The dissociation constant (Kd) and maximum binding (Bmax) for the IgY-RBC interaction was determined using the Ligand Binding macro in SigmaPlot 8.0.

2.9. Estimation of parasitemia by flow cytometry

Plasmodium falciparum-infected RBCs, either unsynchronized or synchronized using sorbitol, were fixed with freshly prepared 1% paraformaldehyde in PBS for 1h at RT. A 25 μL aliquot of the fixed sample was incubated with a 500 μL solution of cell-permeant nucleic acid dye, SYTO-13 (Invitrogen) in PBS for 15 min at RT. SYTO-13 was used at a single final concentration (50 or 100 nM) or a range of final concentrations (0–200 nM). To optimize assay conditions, SYTO-13 samples were analyzed by flow cytometry as previously described [48]. The SYTO-13 green fluorescence was detected using a 530 nm, 20 nm-bandwidth band-pass filter. The flow cytometry software package FCS Express (DeNovo Software) was used for analysis and display of data. Five thousand events were collected and a display of forward versus side scatter was used to define a gate of RBCs. The percentage of cells with green fluorescence above background was analyzed from a density plot showing side scatter on the x-axis and green fluorescence intensity on the y-axis (Fig. 4C) or a one-parameter histogram representing green fluorescence intensity on a logarithmic scale (Fig. 5). Uninfected RBCs were used as control. Assay conditions optimized for estimating parasitemia were reproducible using FACSCalibur as described above (data not shown). The accuracy of estimating parasitemia by our flow cytometry

method was compared with the conventional visual counting method using Giemsa-stained thin smears under a microscope. The two methods gave comparable parasitemia (data not shown).

2.10. RBC invasion inhibition assay

P. falciparum fraction enriched with late-stage trophozoites (>90% enrichment using 63% Percoll) from a sorbitol-synchronized culture was returned to culture by incubating the parasites with fresh normal or Neu-treated human RBCs in a 96-well microplate (final, 2% hematocrit, 1.5–3.5% parasitemia). An aliquot of anti-5C and/or anti-6A IgY antibodies (as inhibitor) passed through a 0.2 micron filter was added to the culture medium. For concentration-dependent inhibition assays, final IgY concentrations used for each preimmune IgY (control), anti-5C IgY, and anti-6A IgY antibodies were 25, 50, 100, and 200 μg/ml. Samples containing a 1:1 mixture of two IgY antibodies were prepared by adding each IgY at 25, 50, 100, and 200 μg/ml final concentrations. A control sample having no IgY antibodies was included. For the invasion phenotype-specific inhibition study, anti-5C IgY, anti-6A IgY, or preimmune IgY were used at the 100 μg/ml final concentration. The assay was allowed to continue for 20–22 hours under standard *P. falciparum* culture conditions and stopped by treating the samples with freshly made 1% paraformaldehyde as mentioned above. Upon collecting 10,000 events using FACSCalibur, parasitemia for each sample was determined based on the newly formed ring-stage parasites at the 50 nM concentration of SYTO-13. For the invasion phenotype-specific inhibition study using recombinant proteins, 8 μM GST-5ABC or GST (control) was added as the inhibitor. A similar protocol was used for measuring the invasion inhibitory effect of Trx-RhopH3-C. The invasion assay was carried out as described above. At the end of the assay, thin smears made from each sample were stained with Giemsa and analyzed visually under a microscope at 100X magnification. Approximately 1,500 cells were counted for each sample and parasitemia estimated based on the number of newly formed ring-stage parasites. All assays were carried out in triplicates and data plotted as percent invasion inhibition (mean ± s.e.). Student's *t*-test was used to compare the mean.

3. Results

3.1. Generation and specificity of chicken IgY antibodies reacting to human RBC Band 3

We generated antibodies against the 5C and 6A regions of human RBC band 3 (Fig. 1). These two regions are thought to shape the core of the band 3 invasion receptor based on our earlier studies [29–31], and have been predicted to adopt extracellular orientation in some topology models [43, 49, 50]. Because human and mouse band 3 polypeptides share very high sequence identity in these regions (Fig. 1A), we had little success in inducing immune response against human 5C or 6A sequences in mice. However, we succeeded in producing anti-5C and anti-6A antibodies in chicken egg yolk using short peptides derived from human 5C and 6A as immunogens. Antibody titers were relatively low for both 5C and 6A based on ELISA even after several injections (data not shown), presumably due to high sequence homology in these regions of band 3 between human and chicken.

Affinity-purified anti-5C and anti-6A IgY antibodies reacted specifically to recombinant proteins GST-5ABC and GST-6A, respectively, by Western blot (Fig. 1B). Further, anti-6A specifically recognized band 3 in RBC ghosts prepared from normal human RBCs (Fig. 1C). However, anti-5C IgY failed to react to band 3 in the normal RBC ghosts sample in Western blot (Fig. 1C). Interestingly, when the RBC ghosts sample was prepared from human RBCs pretreated with neuraminidase (Neu) to remove sialic acid residues from the cell surface (Fig. 1D), the anti-5C IgY reactivity to band 3 was restored under the same conditions (Fig. 1C). Although the precise reason of this differential reactivity response is not yet known, one may speculate that the sialic acid residues on co-migrating sialoglycoproteins may suppress the accessibility of anti-5C IgY to its 5C epitope on band 3 under these Western blotting conditions. Sialic acid residues had no appreciable effect on the reactivity of anti-6A IgY antibodies to band 3 in Western blot (Fig. 1C). As positive control, a monoclonal antibody (mAb) against the N-terminal cytoplasmic domain of human band 3 (Sigma) was used to detect band 3 in normal and Neu-treated RBC ghosts. Purified preimmune control IgY showed no reactivity to either the recombinant proteins (not shown) or the human RBC ghosts proteins (Fig. 1C). These results indicate the generation of two affinity-purified mono-specific antibodies, anti-5C and anti-6A IgY, reactive against human RBC band 3.

3.2. Interaction of anti-Band 3 IgY antibodies with RBCs

Since anti-5C and anti-6A IgY antibodies showed characteristic band 3 recognition patterns on RBC ghosts in Western blot (Fig. 1C), we investigated their band 3-binding properties on intact RBCs. In the first method, we examined the binding of anti-5C IgY and anti-6A IgY to methanol-fixed human RBCs by immunofluorescence microscopy. Normal RBCs (Fig. 2A) as well as sialic acid-depleted RBCs prepared by treating the intact cells with Neu prior to fixing (Fig. 2B) were used. Indirect immunofluorescence assay (IFA) showed that both anti-5C and anti-6A antibodies specifically bound to normal and Neu-treated RBCs. The control preimmune IgY as well as the anti-chicken secondary antibody alone did not show any interaction with fixed RBCs. As a positive control, the anti-band 3 mAb bound to both normal and Neu-treated RBCs as methanol fixation permeabilized the membrane enabling antibodies to react to proteins in the intracellular compartments (Fig. 2A, B). As expected, the monoclonal anti-GPA antibody/clone E4 (Sigma) raised against extracellular residues of human GPA, which are sensitive to sialic acid residues, interacted with normal RBCs bearing sialic acid residues, but not with Neu-treated RBCs where sialic acid residues on the RBC surface have been depleted (Fig. 1D).

In the second method, we examined the binding of anti-5C IgY and anti-6A IgY to RBCs in suspension. Normal and Neu-treated intact human RBCs were reacted with the anti-5C and anti-6A antibodies (100 μg/ml) and analyzed by flow cytometry. As compared to the preimmune IgY control, histograms showed that each anti-5C IgY and anti-6A IgY bound to both normal and Neu-treated RBCs (Fig. 3). The anti-5C IgY showed a stronger interaction with the sialic acid-depleted RBCs than normal RBCs in suspension as indicated by higher fluorescence intensity. This observation is consistent with the earlier Western blot result (Fig. 1C) where the reactivity of anti-5C IgY to band 3 in the RBC ghosts was apparent only in the Neu-treated RBCs. The anti-band 3 mAb reactive to the N-terminal cytoplasmic

domain of band 3 did not bind to either normal or Neu-treated RBCs indicating that the cells were fully intact (Fig. 3). The anti-GPA mAb reactive to surface residues of human GPA bound to normal RBCs but not with Neu-treated RBCs consistent with the IFA results (Fig. 3). These results demonstrate that the anti-5C and anti-6A IgY antibodies react to the extracellular epitopes of band 3 on the surface of normal and Neu-treated intact RBCs.

3.3. Concentration-dependent binding of anti-Band 3 IgY antibodies to RBCs

To quantitatively characterize the interaction of IgY antibodies with intact RBCs, we carried out a concentration-dependent binding of the antibodies using the above flow cytometry method. The data presented as mean fluorescence intensity versus IgY concentration showed that the binding of anti-5C and anti-6A IgY to intact human RBCs is indeed concentration dependent in both normal and Neu-treated cells (Fig. 4A, B). The non-specific binding of preimmune IgY to RBCs was negligible. In normal RBCs, the maximum binding (Bmax) for anti-5C IgY was significantly lower as compared to Neu-treated RBC samples (Table 1). The dissociation constant (Kd), however, remained relatively unchanged in both RBC samples. In contrast, Neu treatment did not have any significant effect on the binding of anti-6A IgY to or dissociation of the IgY from intact RBCs (Fig. 4B). Together, data from Western blotting, immunofluorescence microscopy, and flow cytometry provide compelling evidence that the 5C and 6A regions of band 3 are exposed on the surface of normal human RBCs. Removing sialic acid residues from the cell surface by the Neu treatment of intact RBCs enhances the recognition of the band 3 epitopes, particularly by the anti-5C IgY. Interestingly in our previous study [29], the rate of binding of *P. falciparum* $MSP1_{19}$ and $MSP1_{42}$ to native band 3 on the RBC surface increased when sialic acid residues were removed from the RBC surface by Neu treatment.

3.4. Flow cytometry analysis of parasitemia using SYTO-13

To analyze a large number of samples generated from the RBC reinvasion assay by a reliable and convenient method, we developed a new flow cytometry method as described in the methods section. This method uses cell-permeant nucleic acid dye SYTO-13 (Invitrogen) to accurately estimate parasitemia in the assay samples (Fig. 5). Because it is not necessary to permeabilize the cells for SYTO-13 to function properly, parasites and RBCs in the sample remain much more stable especially from cell lysis for a prolonged time (over 3 days). SYTO-13 is a green fluorescent dye having absorption and emission at 488 nm and 509 nm, respectively, which is suitable for a large selection of commonly used instruments. In contrast, the vital dye Hoechst [51] often used to stain stage-specific malaria parasites requires a flow cytometer equipped with a UV laser. SYTO-13 has high molar absorption (>50,000 $cm^{-1}M^{-1}$) giving low intrinsic fluorescence associated with the background. These salient features of SYTO-13 allowed analysis to readily distinguish different populations of stage-specific parasites from uninfected RBCs in the *P. falciparum* culture using a flow cytometer (Fig. 4C). Other nucleic acid dyes such as Acridine Orange, Thiazole Orange, YOYO-1, YO-PRO-1, and DRAQ5 did not give satisfactory results in our hands. We found that 50 nM SYTO-13 gave an excellent distinction of cell populations between uninfected RBCs and infected RBCs at the ring, trophozoite, and schizont stages, with relatively low background fluorescence (Fig. 4C). The parasitemia estimated using this

method was consistent with the visual counting method using Giemsa-stained thin smears by microscopy (data not shown).

3.5. Blocking P. falciparum invasion in human RBCs using anti-band 3 IgY

Since the binding of anti-5C and anti-6A IgY antibodies to the RBC surface was concentration-dependent, we investigated whether these antibodies would block the reinvasion of RBCs by *P. falciparum* when added to the culture medium. The invasion blocking assay was carried out in the *P. falciparum* (3D7 strain) culture as described [29] using mono-specific anti-5C IgY and anti-6A IgY, either independently or together. The range of IgY concentrations used was similar to the above RBC binding assay. Assay mixtures were analyzed by the above flow cytometry method to quantify newly formed ring-stage parasites and calculate percent parasitemia for each sample (Table 2). To visualize the invasion blocking effect of IgY antibodies, results are presented as the percent inhibition of invasion at a given IgY concentration, by taking the preimmune IgY sample at the equivalent concentration as 0% inhibition (or 100% invasion). In both normal and sialic acid-depleted RBC samples, anti-5C IgY was superior in blocking RBC invasion as compared to anti-6A IgY (Fig. 6A, B). Consistent with its RBC binding property, the rate of invasion inhibition for anti-5C IgY was significantly higher (about 2–3 fold) in the sialic acid-depleted RBCs throughout the IgY concentrations. At 200 μg/ml IgY concentration, the anti-5C IgY blocked RBC invasion by 58% as compared to the preimmune IgY, which had no detectable effect on invasion at all concentrations. Although the Bmax for anti-5C IgY binding to normal RBCs was about two-fold less than for anti-6A IgY (Table 1), the rate of RBC invasion inhibition for anti-5C IgY was about two-fold higher than for anti-6A IgY (Fig. 6A). No accumulation of trophozoites and schizonts was observed during the course of the assay, indicating that the addition of antibodies to the culture medium at the trophozoite stage did not affect intracellular maturation and release of the parasites.

When both anti-5C and anti-6A antibodies were added to the culture medium as a 1:1 mixture, an additive effect was observed (Fig. 6, Table 2). It was also evident that this additive effect was not simply due to the doubling of the total IgY concentration. For example, in normal RBC samples, 100 μg/ml anti-5C IgY produced 18% invasion inhibition, while a mixture of 50 μg/ml anti-5C IgY and 50 μg/ml anti-6A IgY gave 29% inhibition. Similarly, doubling the anti-5C IgY concentration from 25 to 50 μg/ml increased the inhibition rate from 12% to 29% inhibition in Neu-treated RBC samples, but adding 25 μg/ml of each IgY as a mixture resulted in only 20% invasion inhibition. These results suggest that each anti-5C and anti-6A IgY plays an important role in blocking RBC invasion by *P. falciparum*. The rate at which each anti-5C IgY and anti-6A IgY binds to RBCs (Fig. 4A, B) and blocks RBC invasion (Fig. 6A, B) over a similar range of IgY concentrations appear to have a close resemblance. Both the binding of and invasion inhibition by each IgY increased at a rapid rate until about 50 μg/ml concentration. However, the binding and the inhibition slowed down significantly starting at about 100 μg/ml of IgY and reached near maximum at 200–250 μg/ml. These similar rate profiles suggest that the invasion blocking effect of the anti-band 3 IgY antibodies correlates with the binding of these antibodies to their respective epitopes, the 5C and 6A regions of band 3 on the human RBC surface.

3.6. Invasion phenotype-specific inhibition of RBC invasion

In our previous studies, we showed that 5C and 6A regions of RBC band 3 function as an invasion receptor interacting with *P. falciparum* merozoite surface proteins, $MSP1_{42}$/$MSP1_{19}$ and MSP9 by a SAID mechanism [29, 30]. In this study, our data show that both anti-5C and anti-6A antibodies blocked RBC invasion by the *P. falciparum* 3D7 strain, which favors the SAID invasion pathway (Fig. 6). Hence, we asked whether the invasion-blocking function of anti-5C and anti-6A antibodies is limited to a specific invasion phenotype of *P. falciparum*. To investigate this possibility, we carried out the RBC invasion assays using 3D7 and 7G8 strains representing the SAID invasion phenotype, and FCR3 and Dd2 strains representing the SAD invasion phenotype. The concentration of IgY antibodies added as inhibitors in the assay was 100 μg/ml. Normal and sialic acid-depleted (Neu-treated) RBCs were used. Newly formed ring-stage parasites were quantified and parasitemia determined for each assay sample (Table 3) using the flow cytometry method. When the data are presented as percent inhibition of RBC invasion by taking the preimmune IgY control as 0% inhibition, it was evident that anti-5C IgY blocked RBC invasion by the SAID invasion phenotype of *P. falciparum* in both normal and sialic acid-depleted RBC samples (Table 3) (Fig. 7). However, the effect of anti-5C IgY on the SAD invasion phenotype was marginal in both RBC types. In comparison, the anti-6A IgY antibodies showed a relatively weak, nevertheless, significant inhibitory effect on RBC invasion by the SAID invasion phenotype particularly in Neu-treated samples (Table 3). In normal RBC samples, anti-6A IgY alone had little effect on blocking RBC invasion by the either invasion phenotype (Table 3). These results, obtained at 100 μg/ml IgY concentration, are consistent with experiments over a range of IgY concentrations using only the 3D7 strain (Fig. 6).

Since the anti-5C IgY antibody showed a significant inhibitory effect on the invasion of RBCs by the SAID invasion phenotype, we asked whether the human RBC band 3 peptide, 5ABC, would have a similar invasion blocking effect and invasion phenotype specificity. The invasion blocking mechanism for the 5ABC peptide is thought to be distinct from anti-5C IgY. The 5ABC peptide mimicking the band 3 receptor is expected to interact directly with the parasite ligand(s) in competition with band 3, whereas anti-5C IgY would bind to band 3 epitopes and block the band 3 invasion receptor function. However, we anticipated a similar result because in principle both types of inhibition approaches would disrupt interaction between the host receptor band 3 and the parasite ligand(s) during RBC invasion. Considering the mechanism of invasion inhibition by the 5ABC peptide, it was not necessary to use sialic acid-depleted RBCs. Thus, RBC invasion assays were carried out using only normal RBCs in *P. falciparum* cultures containing 3D7, 7G8, FCR3, and Dd2 strains. Soluble GST-5ABC was used as the inhibitor and GST as control each at 8 μM concentration. The results are plotted as percent inhibition of RBC invasion taking the GST control as 0%. Invasion inhibition by the 5ABC peptide was strikingly significant in the SAID invasion phenotype of *P. falciparum* (48–65% inhibition), while it was marginal in the SAD invasion phenotype (<10% inhibition) (Fig. 6C). No accumulation of trophozoites and schizonts was observed in any samples during the course of the assay (data not shown) indicating that recombinant proteins, GST-5ABC and GST did not affect intracellular maturation and release of the parasites. Together, these results indicate that 5C and 6A regions of human band 3 are exposed on the RBC surface and serve as a host invasion

receptor predominantly in the SAID invasion pathway. It appears that the 5C region in particular is an exceptionally important part of the band 3 invasion receptor (Fig. 6D).

3.7. Interaction of Plasmodium falciparum RhopH3 with human RBC Band 3

Identification of the 5ABC region of host RBC band 3 as an invasion receptor raised the possibility that the parasite might utilize multiple ligands to interact with this region, either directly or indirectly to facilitate pathogen entry into host cells. To test this possibility, we performed a yeast two-hybrid screen of a *P. falciparum* cDNA library (3D7, a SAID strain) using the 5ABC peptide (amino acids 720-761) of human RBC band 3 as bait [30]. Sequencing of at least three clones revealed the C-terminal region of RhopH3 protein (amino acids 431-876) as the binding segment (Fig. 8A). RhopH3 is a component of the high molecular weight complex (HMW) of rhoptry proteins [52]. Although the precise membrane topology of RhopH3 is not yet known, multiple predictive models indicate several short transmembrane domains embedded within the primary structure of RhopH3 [47]. The ConPred II [53] program predicted a transmembrane region (amino acids 593-613) within the yeast two-hybrid clone of RhopH3 (Fig. 8A). Thus, we excluded the predicted transmembrane domain(s) to express a shorter segment of RhopH3 (amino acids 620-897), termed RhopH3-C, in order to validate its biochemical interaction with the 5ABC peptide of RBC band 3 (Fig. 8A). The RhopH3-C segment was expressed as a fusion protein containing Trx and His tags with an apparent mass of 52 kDa (Trx-RhopH3-C) (Fig. 8B). In addition, we developed an affinity-purified polyclonal anti-peptide (amino acids 876-892; Fig. 8A) antibody against RhopH3 to confirm the identity and intactness of recombinant RhopH3-C protein (Fig. 8C). The 5ABC peptide of band 3 was expressed as GST fusion protein of 32 kDa (Fig. 1B). Solution binding assays confirmed specific biochemical interaction between Trx-RhopH3-C and 5ABC peptide immobilized to glutathione beads (Fig. 9A). The affinity of Trx-RhopH3-C interaction with 5ABC, as measured by a quantitative ELISA, yielded a Kd value of 183 nM ± 0.111 (Fig. 9B). A truncated version of 5ABC peptide (Δ5ABC), lacking the last 19 amino acids, partially lost Trx-RhopH3-C binding activity (Fig. 9A). Together, these results indicate that the C-terminal segment of RhopH3 directly interacts with the 5ABC region of human RBC band 3.

3.8. Biochemical interactions between RhopH3, MSP1, and Band 3

A global interaction network analysis of *P. falciparum* predicted a major role of MSP1 by virtue of its interactions with more than 80 proteins in the malaria genome [32]. Consistent with the interaction network, the C-terminal 19 kDa segment of MSP1 ($MSP1_{19}$) interacted with the C terminal segment (amino acids 734-865) of RhopH3 [32, 47]. To assess the inter-dependence of biochemical interactions between RhopH3, MSP1, and band 3, we expressed $MSP1_{19}$ (amino acids 1665-1760) as a fusion with maltose binding protein (MBP) (Fig. 8B). Amylose beads with immobilized MBP-$MSP1_{19}$ specifically bound soluble Trx-RhopH3-C indicating a direct biochemical interaction (Fig. 9C). The affinity of Trx-RhopH3-C interaction with MBP-$MSP1_{19}$, as measured by an ELISA, yielded a Kd value of 390 nM ± 0.032 (Fig. 9D). Since RhopH3 interacts directly with both MSP1 and 5ABC and $MSP1_{19}$ is known to bind to 5ABC, we developed a competitive binding assay to evaluate the inter-dependence of RhopH3 and $MSP1_{19}$ interactions with 5ABC. For this assay, $MSP1_{19}$ was expressed as a Trx fusion protein (Fig. 8B), and ternary interactions between MSP_{19},

RhopH3, and 5ABC were examined (Fig. 10A). Glutathione beads saturated with GST-5ABC were incubated with an equimolar concentration of Trx-RhopH3-C to allow saturation binding (Fig. 10B). Trx-$MSP1_{19}$ was then added at increasing molar ratios (1, 2.5, 5, and 10) to compete off bound Trx-RhopH3-C from immobilized 5ABC (Fig. 10B). $MSP1_{19}$ progressively displaced RhopH3 from 5ABC at increasing molar concentrations (Fig. 10B). At 10 molar excess of $MSP1_{19}$, the $MSP1_{19}$ and RhopH3-C formed a ternary complex with 5ABC suggesting a concentration dependent occupancy of the binding sites under these conditions. Additionally, a parasite supernatant binding assay was performed to test for endogenous RhopH3 binding to 5ABC. Parasite supernatant demonstrated a very low abundance of endogenous RhopH3, detectable only by immunoblotting; however, this endogenous protein specifically bound 5ABC protein immobilized on GST beads (Fig. 9E). Thus, in addition to recombinant RhopH3-C, native RhopH3 demonstrates a specific interaction with 5ABC.

3.9. RhopH3 inhibits Plasmodium falciparum invasion in Human RBCs

Trx-RhopH3-C binds specifically to human RBCs in a solution binding assay (Fig. 11A). Since Trx-RhopH3-C binds to the 5ABC region of band 3 (Fig. 9A), its interaction with intact RBCs was unaffected upon treatment of RBCs with either neuraminidase (Neu) or trypsin (T) (Fig. 11A). In fact, binding of Trx-RhopH3-C to RBCs was slightly increased upon trypsin treatment of RBCs, presumably due to the removal of glycophorin A from the glycophorin A-band 3 complex (Fig. 11A). The chymotrypsin treatment of RBCs is known to cleave RBC band 3 into two lower MW bands that would retain the 5 ABC peptide sequence (Fig. 11B, C). Indeed, chymotrypsin treatment (C) of RBCs did not affect the Trx-RhopH3-C interaction under the same assay conditions (Fig. 11A). Moreover, Trx-RhopH3-C binding to RBCs that were sequentially treated with trypsin, chymotrypsin, and neuraminidase (TT) essentially remained unchanged (Fig. 11A). These results suggest that RhopH3 binds to RBCs in a sialic acid-independent manner. We then tested the inhibitory activity of Trx-RhopH3-C on *P. falciparum* (3D7) invasion in human RBCs. Because of the technical limitations of limited solubility and stability, the Trx-RhopH3-C fusion protein was used only at two concentrations (2.5 and 5 μM) in the reinvasion assay. Relative to Trx, the addition of Trx-RhopH3-C resulted in significant inhibition of invasion at both 2.5 and 5.0 μM concentrations (Fig. 11D). Again, the morphology and maturation of intra-erythrocytic parasites was not affected by the presence of Trx-RhopH3-C (data not shown). Future mapping studies of the band 3 binding site within RhopH3-C is required to identify high affinity binding peptides for achieving maximum inhibition of parasite invasion at high molar concentrations. Together, these results identify the 5ABC region of RBC band 3 as the first host receptor for *P. falciparum* RhopH3 that mediates sialic acid independent invasion of malaria parasite in human red blood cells.

4. Discussion

Host receptors are thought to mediate initial attachment, reorientation, and penetration of merozoites in RBCs by regulating signaling of specifically timed molecular steps of the invasion process. Over the last three decades or so, significant progress has been made towards the functional identification of *Plasmodium* proteins/ligands localized to the

merozoite surface, rhoptries, and micronemes that are known to interact with host receptors during invasion [2, 54]. In contrast, molecular understanding of the cognate receptors on host RBCs is relatively limited. Naturally occurring mutations in human genes encoding RBC membrane proteins have been informative [1]; however, these abnormal RBCs are rare and their utility is limited to certain non-lethal hereditary genetic mutations. Targeted mutations of genes encoding RBC membrane proteins in mice are technically challenging and time consuming. Moreover, this approach suffers from the criticism that the receptor-ligand interaction(s) governing murine malaria parasites might be different from *P. falciparum*. More recently, genetic manipulation of erythroid progenitors has been used to interrogate novel host-parasite interactions [28, 55]. However, the potential of this approach remains to be validated by the identification of new ligand-receptor interactions in future studies.

Using molecular and biochemical approaches, we previously identified human RBC band 3 as an important host invasion receptor for *P. falciparum*, binding to a parasite co-ligand complex containing $MSP1_{19}$ (or $MSP1_{42}$) and MSP9 [29–31]. The core of the band 3 invasion receptor includes two putative exofacial regions designated as 5C and 6A. The 5C peptide is part of the 5ABC region of band 3 as described previously [29]. In this study, using mono-specific anti-5C IgY and anti-6A IgY antibodies, we demonstrate that 5C and 6A (or considerable parts of these two regions) are indeed exposed on the normal human RBC membrane. Since each 5C and 6A shares almost identical amino acid sequence between human and mouse (Fig. 1A), our failed attempts to generate antibodies in mice against these two regions support the notion that 5C and 6A peptides of band 3 are also exposed on the mouse RBC surface. The flow cytometry analysis of intact RBCs (Fig. 4) suggested that the epitope(s) for anti-5C IgY is masked to some extent by sialic acid residues on the normal human RBC surface, because the antibody showed increased reactivity towards its epitope(s) on sialic acid-depleted cells. It is unlikely that removing negatively charged sialic acid residues from the cell surface would affect the normal folding of RBC membrane proteins for the following two reasons: First, in the concentration-dependent invasion inhibition assay (Table 2), preimmune IgY control samples for normal and Neu-treated RBCs retained a similar level of parasitemia (5.6%–6.6%) in all IgY concentrations (0–200 μg/ml). Second, the binding of anti-6A IgY to its epitope(s) on the intact RBC surface was not affected as judged by the Bmax (Table 1). Native band 3 is folded in the RBC membrane mainly as homo-dimers and tetramers, which are part of a larger protein complex [56]. It is well established that GPA, heavily glycosylated with sialic acid residues, interacts directly with band 3 [57–59]. Therefore, we postulate a sub-population of band 3 dimers and/or tetramers on the human RBC membrane contains 5C that is fully exposed, whereas the remaining population has 5C masked by sialic acid residues branched out from the surrounding RBC membrane proteins (e.g., GPA). Interestingly, sialic acid content of band 3 decreases during erythrocyte aging [60]. Moreover, it has been hypothesized that oxidative stress may influence this desialylation process. And while an altered glycosylation status of band 3 did not show a significant hematological effect *in vivo*, evidence exists that glycosylation of band 3 is inhibitory towards oxidative cross-linking [61, 62].

This view is supported by the equilibrium binding parameters estimated for anti-5C IgY in normal and Neu-treated RBC samples (Table 1), in which the Kd remained relatively unchanged despite three-fold increase in the Bmax. These observations further support our conclusion that the epitope(s) for mono-specific anti-5C IgY antibody is exposed on the surface of normal RBCs. Our findings provide direct evidence for the exofacial folding of 5C and 6A regions of band 3 in the normal human RBC membrane, thus lending support to multiple topology models for human RBC band 3 delineating the TM10-12 segments of the membrane domain [42–46].

Interestingly, the level of inhibition between the SAID and SAD invasion phenotypes was much more significant in the sialic acid-depleted RBCs (Fig. 6C). We believe this is mainly because the alternate SAD invasion pathway utilizing RBC sialic acid residues has been practically eliminated by the Neu treatment of the cells. Under such conditions, 3D7 and 7G8 strains would have no option to switch to the alternate invasion pathway even in the presence of a pressuring effect of anti-5C IgY, but continue to rely on the SAID invasion pathway. This appears to be the case in the 3D7 and 7G8 strains because the preimmune control samples showed no appreciable difference in the invasion rate between normal and Neu-treated RBCs (Table 3). Moreover, the depletion of sialic acid residues increases the anti-5C IgY binding capacity of RBCs (Figs. 1,2) and in turn provides better protection from invasion by the SAID invasion phenotype (Fig. 6B). Taken together, sialic acid-depleted RBCs provide a better model for determining the effect of anti-band 3 antibodies on the SAID invasion phenotype and/or pathway.

The mechanism by which *P. falciparum* invades human RBCs is more complex than what is known for other *Plasmodium* species, as two alternate (SAD and SAID) invasion pathways have been implicated [6, 7]. Moreover, these two broadly defined invasion pathways seem to tolerate additional complexity, because there are further disparities within each SAD and SAID invasion pathway characterized by the sensitivity of the host invasion receptor function to proteolytic activities [5, 13, 24]. In our invasion inhibition assays using the 3D7 strain, the mixture of anti-5C and anti-6A IgY antibodies at a near saturating concentration (200 μg/ml/each IgY) was able to block RBC invasion only by about 33% and 65% in normal and sialic acid-depleted RBC samples, respectively (Fig. 6). These results, together with our invasion phenotype-specific inhibition study (Figs. 6 and 7), suggest that band 3 is a major host invasion receptor in the SAID invasion pathway, but one or more host receptor is also taking part in this pathway. Moreover, in sialic acid-depleted RBC samples, the invasion rates for FCR3 and Dd2 strain (SAD invasion phenotype) were reduced to 49% and 56%, respectively, as compared to normal RBC samples, when preimmune IgY antibodies (control) were present in the culture medium (Table 3). As neither anti-5C nor anti-6A antibodies showed the invasion blocking effect at a significant level, our data suggest that the newly emerged invasion phenotype does not rely on the host band 3 receptor during RBC invasion. As pointed out above, other alternate host receptor could be providing a dominant interaction in order for FCR3 and Dd2 strains to invade Neu-treated RBCs. It has been suggested that a molecular hierarchy of parasite ligands set by an unknown mechanism may determine the dominant interaction(s) between a particular *P. falciparum* clone and host RBCs during invasion [63].

The vast abundance and specificity of band 3 in the RBC membrane suggest that this multi-transmembrane protein could serve as an anchor for multiple malaria parasite proteins, facilitating a complex merozoite invasion cascade in host RBCs. Band 3 exists in multiple subpopulations in the host membrane, including mobile and anchored dimers/tetramers as well as a tightly bound complex of band 3 with glycophorin A [56]. These unique features of band 3 could be exploited by the parasite to engage multiple ligands in a sequential manner to facilitate invasion in RBCs. As part of our long term goal to map the network of parasite invasion ligands that interact with host band 3-glycophorin A complex, we identified the carboxyl-terminus of *P. falciparum* RhopH3 as the ligand interacting with the 5ABC region of human band 3 (Figs. 8 and 9). A direct interaction between RhopH3-C with $MSP1_{19}$ was established (Fig. 9), consistent with our previous findings showing binding of the MSP1-MSP9 complex with Band 3 [31]. We also show that RhopH3-C binds to intact RBCs and recombinant RhopH3-C inhibits parasite invasion in human RBCs (Fig. 11). Our results are consistent with previous findings that MSP1 participates in a macro-protein complex of *P. falciparum* schizont-merozoite ligands MSP-3, MSP-6, MSP-7, MSP-9, RhopH3, RhopH1/Clag, RAP-1, RAP-2, and two putative RAP domain containing proteins [32]. Recent evidence showing antibodies against RhopH3 inhibit merozoite invasion [47] is consistent with our finding of similar inhibitory effect of recombinant RhopH3-C on merozoite invasion in human RBCs (Fig. 11). However, in contrast to the same study [47], our findings show that RhopH3-C binding to RBCs is not affected in the trypsin-treated RBC (Fig. 11). This observation could be explained due to the use of MBP-RhopH3-C fusion in the previous study [47] and the Trx-RhopH3-C fusion in this study. In fact, our attempts to use MBP-RhopH3-C failed to ensure specificity of interaction with intact RBCs, presumably due to the non-specific interaction of maltose binding protein (MBP) to related sugar moieties on the surface of human RBCs. Based on these observations, we infer that the use of MBP as affinity tag should be avoided in designing binding assays of fusion proteins with intact RBCs. Together, our findings provide the first evidence that the 5ABC region of band 3 serves as a host receptor for *P. falciparum* RhopH3.

5. Conclusions

In conclusion, this study provides compelling biochemical evidence that specific regions of loops 5 and 6 of human RBC band 3 are exposed and accessible to multiple ligands of *P. falciparum* involved in the SAID invasion pathway. Given the known function of host RBC sialoglycoproteins (GPA, GPB, GPC), complement receptor-1, basigin, and putative receptors W, Y and Z as crucial invasion phenotype-specific receptors [64], future identification of dominant host receptors for prevalent *P. falciparum* invasion phenotypes will provide a better understanding of invasion phenotype-specific host-parasite interactions and the extent of redundancy in the RBC invasion mechanism. Further studies in this direction will facilitate and contribute to the development of an effective malaria vaccine.

Acknowledgments

We are grateful to Howard M. Shapiro and Nancy Perlmutter of the Center for Microbial Cytometry, West Newton, MA 02465 for generously providing technical advice and facilities during the optimization of flow cytometry experiments. We also thank Michael M. Kariuki for technical assistance and advice, and Malaria Research and

Reference Reagent Resource Center for the *Plasmodium falciparum* strains used in the study. This work was supported by National Institutes of Health Grants AI054532 (S.S.O.) and HL060961, HL095050 (A.C.).

Abbreviations

RBC	red blood cell
SAD	sialic acid-dependent
SAID	sialic acid-independent
GPA	glycophorin A
GPB	glycophorin B
GPC	glycophorin C
MSP1	merozoite surface protein 1
MSP9	merozoite surface protein 9
Neu	neuraminidase

References

1. Oh SS, Chishti AH. Host receptors in malaria merozoite invasion. Curr Top Microbiol Immunol. 2005; 295:203–232. [PubMed: 16265892]
2. Cowman AF, Berry D, Baum J. The cellular and molecular basis for malaria parasite invasion of the human red blood cell. J Cell Biol. 2012; 198:961–971. [PubMed: 22986493]
3. Okoyeh JN, Pillai CR, Chitnis CE. Plasmodium falciparum field isolates commonly use erythrocyte invasion pathways that are independent of sialic acid residues of glycophorin A. Infect Immun. 1999; 67:5784–5791. [PubMed: 10531229]
4. Baum J, Pinder M, Conway DJ. Erythrocyte invasion phenotypes of Plasmodium falciparum in The Gambia. Infect Immun. 2003; 71:1856–1863. [PubMed: 12654801]
5. Lobo CA, de Frazao K, Rodriguez M, Reid M, Zalis M, Lustigman S. Invasion profiles of Brazilian field isolates of Plasmodium falciparum: phenotypic and genotypic analyses. Infect Immun. 2004; 72:5886–5891. [PubMed: 15385490]
6. Mitchell GH, Hadley TJ, McGinniss MH, Klotz FW, Miller LH. Invasion of erythrocytes by Plasmodium falciparum malaria parasites: evidence for receptor heterogeneity and two receptors. Blood. 1986; 67:1519–1521. [PubMed: 3516259]
7. Dolan SA, Miller LH, Wellems TE. Evidence for a switching mechanism in the invasion of erythrocytes by Plasmodium falciparum. J Clin Invest. 1990; 86:618–624. [PubMed: 2200806]
8. Soubes SC, Wellems TE, Miller LH. Plasmodium falciparum: a high proportion of parasites from a population of the Dd2 strain are able to invade erythrocytes by an alternative pathway. Exp Parasitol. 1997; 86:79–83. [PubMed: 9149243]
9. Binks RH, Conway DJ. The major allelic dimorphisms in four Plasmodium falciparum merozoite proteins are not associated with alternative pathways of erythrocyte invasion. Mol Biochem Parasitol. 1999; 103:123–127. [PubMed: 10514089]
10. Camus D, Hadley TJ. A Plasmodium falciparum antigen that binds to host erythrocytes and merozoites. Science. 1985; 230:553–556. [PubMed: 3901257]
11. Orlandi PA, Klotz FW, Haynes JD. A malaria invasion receptor, the 175-kilodalton erythrocyte binding antigen of Plasmodium falciparum recognizes the terminal Neu5Ac(alpha 2-3)Gal-sequences of glycophorin A. J Cell Biol. 1992; 116:901–909. [PubMed: 1310320]
12. Sim BK, Chitnis CE, Wasniowska K, Hadley TJ, Miller LH. Receptor and ligand domains for invasion of erythrocytes by Plasmodium falciparum. Science. 1994; 264:1941–1944. [PubMed: 8009226]

13. Duraisingh MT, Maier AG, Triglia T, Cowman AF. Erythrocyte-binding antigen 175 mediates invasion in Plasmodium falciparum utilizing sialic acid-dependent and -independent pathways. Proc Natl Acad Sci U S A. 2003; 100:4796–4801. [PubMed: 12672957]

14. Gilberger TW, Thompson JK, Triglia T, Good RT, Duraisingh MT, Cowman AF. A novel erythrocyte binding antigen-175 paralogue from Plasmodium falciparum defines a new trypsin-resistant receptor on human erythrocytes. J Biol Chem. 2003; 278:14480–14486. [PubMed: 12556470]

15. Mayer DC, Cofie J, Jiang L, Hartl DL, Tracy E, Kabat J, Mendoza LH, Miller LH. Glycophorin B is the erythrocyte receptor of Plasmodium falciparum erythrocyte-binding ligand, EBL-1. Proc Natl Acad Sci U S A. 2009; 106:5348–5352. [PubMed: 19279206]

16. Li X, Marinkovic M, Russo C, McKnight CJ, Coetzer TL, Chishti AH. Identification of a specific region of Plasmodium falciparum EBL-1 that binds to host receptor glycophorin B and inhibits merozoite invasion in human red blood cells. Mol Biochem Parasitol. 2012; 183:23–31. [PubMed: 22273481]

17. Maier AG, Duraisingh MT, Reeder JC, Patel SS, Kazura JW, Zimmerman PA, Cowman AF. Plasmodium falciparum erythrocyte invasion through glycophorin C and selection for Gerbich negativity in human populations. Nat Med. 2003; 9:87–92. [PubMed: 12469115]

18. Lobo CA, Rodriguez M, Reid M, Lustigman S. Glycophorin C is the receptor for the Plasmodium falciparum erythrocyte binding ligand PfEBP-2 (baebl). Blood. 2003; 101:4628–4631. [PubMed: 12576308]

19. Mayer DC, Kaneko O, Hudson-Taylor DE, Reid ME, Miller LH. Characterization of a Plasmodium falciparum erythrocyte-binding protein paralogous to EBA-175. Proc Natl Acad Sci U S A. 2001; 98:5222–5227. [PubMed: 11309486]

20. Narum DL, Fuhrmann SR, Luu T, Sim BK. A novel Plasmodium falciparum erythrocyte binding protein-2 (EBP2/BAEBL) involved in erythrocyte receptor binding. Mol Biochem Parasitol. 2002; 119:159–168. [PubMed: 11814568]

21. Triglia T, Duraisingh MT, Good RT, Cowman AF. Reticulocyte-binding protein homologue 1 is required for sialic acid-dependent invasion into human erythrocytes by Plasmodium falciparum. Mol Microbiol. 2005; 55:162–174. [PubMed: 15612925]

22. Hadley TJ, Klotz FW, Pasvol G, Haynes JD, McGinniss MH, Okubo Y, Miller LH. Falciparum malaria parasites invade erythrocytes that lack glycophorin A and B (MkMk). Strain differences indicate receptor heterogeneity and two pathways for invasion. J Clin Invest. 1987; 80:1190–1193. [PubMed: 3308959]

23. Dolan SA, Proctor JL, Alling DW, Okubo Y, Wellems TE, Miller LH. Glycophorin B as an EBA-175 independent Plasmodium falciparum receptor of human erythrocytes. Mol Biochem Parasitol. 1994; 64:55–63. [PubMed: 8078523]

24. Duraisingh MT, Triglia T, Ralph SA, Rayner JC, Barnwell JW, McFadden GI, Cowman AF. Phenotypic variation of Plasmodium falciparum merozoite proteins directs receptor targeting for invasion of human erythrocytes. EMBO J. 2003; 22:1047–1057. [PubMed: 12606570]

25. Kato K, Mayer DC, Singh S, Reid M, Miller LH. Domain III of Plasmodium falciparum apical membrane antigen 1 binds to the erythrocyte membrane protein Kx. Proc Natl Acad Sci U S A. 2005; 102:5552–5557. [PubMed: 15805191]

26. Tham WH, Wilson DW, Lopaticki S, Schmidt CQ, Tetteh-Quarcoo PB, Barlow PN, Richard D, Corbin JE, Beeson JG, Cowman AF. Complement receptor 1 is the host erythrocyte receptor for Plasmodium falciparum PfRh4 invasion ligand. Proc Natl Acad Sci U S A. 2010; 107:17327–17332. [PubMed: 20855594]

27. Spadafora C, Awandare GA, Kopydlowski KM, Czege J, Moch JK, Finberg RW, Tsokos GC, Stoute JA. Complement receptor 1 is a sialic acid-independent erythrocyte receptor of Plasmodium falciparum. PLoS pathogens. 2010; 6:e1000968. [PubMed: 20585558]

28. Crosnier C, Bustamante LY, Bartholdson SJ, Bei AK, Theron M, Uchikawa M, Mboup S, Ndir O, Kwiatkowski DP, Duraisingh MT, Rayner JC, Wright GJ. Basigin is a receptor essential for erythrocyte invasion by Plasmodium falciparum. Nature. 2011; 480:534–537. [PubMed: 22080952]

29. Goel VK, Li X, Chen H, Liu SC, Chishti AH, Oh SS. Band 3 is a host receptor binding merozoite surface protein 1 during the Plasmodium falciparum invasion of erythrocytes. Proc Natl Acad Sci U S A. 2003; 100:5164–5169. [PubMed: 12692305]
30. Li X, Chen H, Oo TH, Daly TM, Bergman LW, Liu SC, Chishti AH, Oh SS. A co-ligand complex anchors Plasmodium falciparum merozoites to the erythrocyte invasion receptor band 3. J Biol Chem. 2004; 279:5765–5771. [PubMed: 14630931]
31. Kariuki MM, Li X, Yamodo I, Chishti AH, Oh SS. Two Plasmodium falciparum merozoite proteins binding to erythrocyte band 3 form a direct complex. Biochem Biophys Res Commun. 2005; 338:1690–1695. [PubMed: 16289042]
32. LaCount DJ, Vignali M, Chettier R, Phansalkar A, Bell R, Hesselberth JR, Schoenfeld LW, Ota I, Sahasrabudhe S, Kurschner C, Fields S, Hughes RE. A protein interaction network of the malaria parasite Plasmodium falciparum. Nature. 2005; 438:103–107. [PubMed: 16267556]
33. Tanner MJ, Martin PG, High S. The complete amino acid sequence of the human erythrocyte membrane anion-transport protein deduced from the cDNA sequence. Biochem J. 1988; 256:703–712. [PubMed: 3223947]
34. Lux SE, John KM, Kopito RR, Lodish HF. Cloning and characterization of band 3, the human erythrocyte anion-exchange protein (AE1). Proc Natl Acad Sci U S A. 1989; 86:9089–9093. [PubMed: 2594752]
35. Low PS. Structure and function of the cytoplasmic domain of band 3: center of erythrocyte membrane-peripheral protein interactions. Biochim Biophys Acta. 1986; 864:145–167. [PubMed: 2943319]
36. Zhang D, Kiyatkin A, Bolin JT, Low PS. Crystallographic structure and functional interpretation of the cytoplasmic domain of erythrocyte membrane band 3. Blood. 2000; 96:2925–2933. [PubMed: 11049968]
37. Lewis IA, Campanella ME, Markley JL, Low PS. Role of band 3 in regulating metabolic flux of red blood cells. Proc Natl Acad Sci U S A. 2009; 106:18515–18520. [PubMed: 19846781]
38. Tanner MJ. The structure and function of band 3 (AE1): recent developments (review). Mol Membr Biol. 1997; 14:155–165. [PubMed: 9491367]
39. Vince JW, Reithmeier RA. Carbonic anhydrase II binds to the carboxyl terminus of human band 3, the erythrocyte C1−/HCO3− exchanger. J Biol Chem. 1998; 273:28430–28437. [PubMed: 9774471]
40. Wang DN, Sarabia VE, Reithmeier RA, Kuhlbrandt W. Three-dimensional map of the dimeric membrane domain of the human erythrocyte anion exchanger, Band 3. EMBO J. 1994; 13:3230–3235. [PubMed: 8045253]
41. Tanner MJ. Molecular and cellular biology of the erythrocyte anion exchanger (AE1). Semin Hematol. 1993; 30:34–57. [PubMed: 8434259]
42. Popov M, Li J, Reithmeier RA. Transmembrane folding of the human erythrocyte anion exchanger (AE1, Band 3) determined by scanning and insertional N-glycosylation mutagenesis. Biochem J. 1999; 339(Pt 2):269–279. [PubMed: 10191257]
43. Kanki T, Sakaguchi M, Kitamura A, Sato T, Mihara K, Hamasaki N. The tenth membrane region of band 3 is initially exposed to the luminal side of the endoplasmic reticulum and then integrated into a partially folded band 3 intermediate. Biochemistry (Mosc). 2002; 41:13973–13981.
44. Zhu Q, Casey JR. The substrate anion selectivity filter in the human erythrocyte Cl−/HCO3− exchange protein, AE1. J Biol Chem. 2004; 279:23565–23573. [PubMed: 15044489]
45. Yamaguchi T, Ikeda Y, Abe Y, Kuma H, Kang D, Hamasaki N, Hirai T. Structure of the membrane domain of human erythrocyte anion exchanger 1 revealed by electron crystallography. J Mol Biol. 2010; 397:179–189. [PubMed: 20100494]
46. Hirai T, Hamasaki N, Yamaguchi T, Ikeda Y. Topology models of anion exchanger 1 that incorporate the anti-parallel V-shaped motifs found in the EM structure. Biochem Cell Biol. 2011; 89:148–156. [PubMed: 21455267]
47. Ranjan R, Chugh M, Kumar S, Singh S, Kanodia S, Hossain MJ, Korde R, Grover A, Dhawan S, Chauhan VS, Reddy VS, Mohmmed A, Malhotra P. Proteome analysis reveals a large merozoite surface protein-1 associated complex on the Plasmodium falciparum merozoite surface. J Proteome Res. 2011; 10:680–691. [PubMed: 21175202]

48. Shapiro HM, Perlmutter NG, Stein PG. A flow cytometer designed for fluorescence calibration. Cytometry. 1998; 33:280–287. [PubMed: 9773891]
49. Popov M, Li J, Reithmeier RA. Transmembrane folding of the human erythrocyte anion exchanger (AE1, Band 3) determined by scanning and insertional N-glycosylation mutagenesis. Biochem J. 1999; 339(Pt 2):269–279. [PubMed: 10191257]
50. Zhu Q, Casey JR. The substrate anion selectivity filter in the human erythrocyte Cl−/HCO3− exchange protein, AE1. J Biol Chem. 2004; 279:23565–23573. [PubMed: 15044489]
51. Janse CJ, van Vianen PH, Tanke HJ, Mons B, Ponnudurai T, Overdulve JP. Plasmodium species: flow cytometry and microfluorometry assessments of DNA content and synthesis. Exp Parasitol. 1987; 64:88–94. [PubMed: 2440713]
52. Kats LM, Black CG, Proellocks NI, Coppel RL. Plasmodium rhoptries: how things went pear-shaped. Trends in parasitology. 2006; 22:269–276. [PubMed: 16635585]
53. Arai M, Mitsuke H, Ikeda M, Xia JX, Kikuchi T, Satake M, Shimizu T. ConPred II: a consensus prediction method for obtaining transmembrane topology models with high reliability. Nucleic Acids Res. 2004; 32:W390–393. [PubMed: 15215417]
54. Cowman AF, Crabb BS. Invasion of red blood cells by malaria parasites. Cell. 2006; 124:755–766. [PubMed: 16497586]
55. Bei AK, Brugnara C, Duraisingh MT. In vitro genetic analysis of an erythrocyte determinant of malaria infection. J Infect Dis. 2010; 202:1722–1727. [PubMed: 20958212]
56. Bruce LJ, Beckmann R, Ribeiro ML, Peters LL, Chasis JA, Delaunay J, Mohandas N, Anstee DJ, Tanner MJ. A band 3-based macrocomplex of integral and peripheral proteins in the RBC membrane. Blood. 2003; 101:4180–4188. [PubMed: 12531814]
57. Nigg EA, Bron C, Girardet M, Cherry RJ. Band 3-glycophorin A association in erythrocyte membrane demonstrated by combining protein diffusion measurements with antibody-induced cross-linking. Biochemistry (Mosc). 1980; 19:1887–1893.
58. Hassoun H, Hanada T, Lutchman M, Sahr KE, Palek J, Hanspal M, Chishti AH. Complete deficiency of glycophorin A in red blood cells from mice with targeted inactivation of the band 3 (AE1) gene. Blood. 1998; 91:2146–2151. [PubMed: 9490702]
59. Auffray I, Marfatia S, de Jong K, Lee G, Huang CH, Paszty C, Tanner MJ, Mohandas N, Chasis JA. Glycophorin A dimerization and band 3 interaction during erythroid membrane biogenesis: in vivo studies in human glycophorin A transgenic mice. Blood. 2001; 97:2872–2878. [PubMed: 11313283]
60. Mehdi MM, Singh P, Rizvi SI. Erythrocyte sialic acid content during aging in humans: correlation with markers of oxidative stress. Disease markers. 2012; 32:179–186. [PubMed: 22377734]
61. Zdebska E, Bader-Meunier B, Schischmanoff PO, Dupre T, Seta N, Tchernia G, Koscielak J, Delaunay J. Abnormal glycosylation of red cell membrane band 3 in the congenital disorder of glycosylation Ig. Pediatric research. 2003; 54:224–229. [PubMed: 12736397]
62. Pantaleo A, Ferru E, Giribaldi G, Mannu F, Carta F, Matte A, de Franceschi L, Turrini F. Oxidized and poorly glycosylated band 3 is selectively phosphorylated by Syk kinase to form large membrane clusters in normal and G6PD-deficient red blood cells. Biochem J. 2009; 418:359–367. [PubMed: 18945214]
63. Baum J, Maier AG, Good RT, Simpson KM, Cowman AF. Invasion by P. falciparum merozoites suggests a hierarchy of molecular interactions. PLoS pathogens. 2005; 1:e37. [PubMed: 16362075]
64. Tham WH, Healer J, Cowman AF. Erythrocyte and reticulocyte binding-like proteins of Plasmodium falciparum. Trends in parasitology. 2012; 28:23–30. [PubMed: 22178537]

Highlights

- RhopH3 binds to the 5ABC region of Band 3
- RhopH3, MSP1-19, and Band 3 form a ternary complex
- Antibodies against the RhopH3 binding region of Band 3 inhibit parasite invasion
- Recombinant RhopH3 inhibits parasite invasion

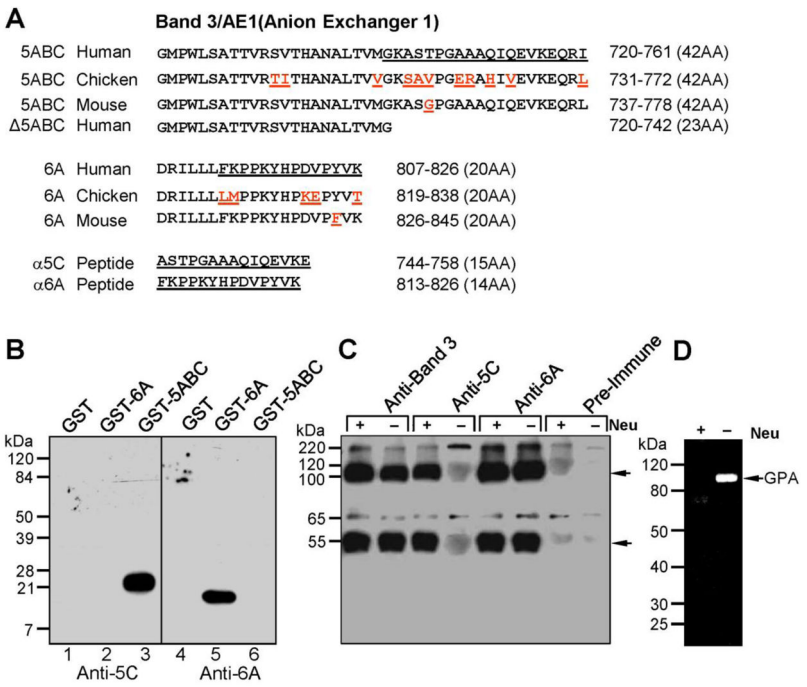

Fig. 1.

Generation of anti-band 3 IgY antibodies. (A) Alignment of the amino acid sequences of 5ABC, Δ5ABC, and 6A regions of human, chicken, and mouse RBC band 3. Chicken and mouse sequences divergent from the human sequence are shown in red and underscored. Peptides patterned on the human 5C and 6A sequence to produce antibodies in chicken are underlined. (B) Western blot showing mono-specific anti-5C (left panel) and anti-6A (right panel) IgY antibodies are reactive against the 5ABC and 6A domain of purified GST-fusion proteins, respectively. Lanes 1 and 4, GST; Lanes 2 and 5, GST-6A, Lanes 3 and 6, GST-5ABC. (C) Western blot showing anti-5C and anti-6A IgY antibodies reacting to full-length band 3 in human RBC ghosts. A truncated band 3 band is also observed. Anti-band 3 mAb against the N-terminal cytoplasmic domain (B3/cd) and preimmune IgY were used as controls. Neu− (no Neu treatment), ghosts from normal human RBCs. Neu+ (Neu treatment), ghosts from neuraminidase-treated intact human RBCs. (D) Staining of a polyacrylamide gel using Glyco-Pro (see Experimental Procedures) to verify the removal of sialic acid residues on the Neu-treated RBC membrane is shown. Neu− and Neu+ lanes are as above. Only in the Neu− lane, a single fluorescent band corresponding to dimeric GPA bearing most of sialic acids on the RBC surface is visible. This band is known to co-migrate with band 3, although not apparent in Coomassie-stained gels [29]. Equal loading of ghost proteins was used in all immunoblotting experiments as observed by Coomassie staining (not shown).

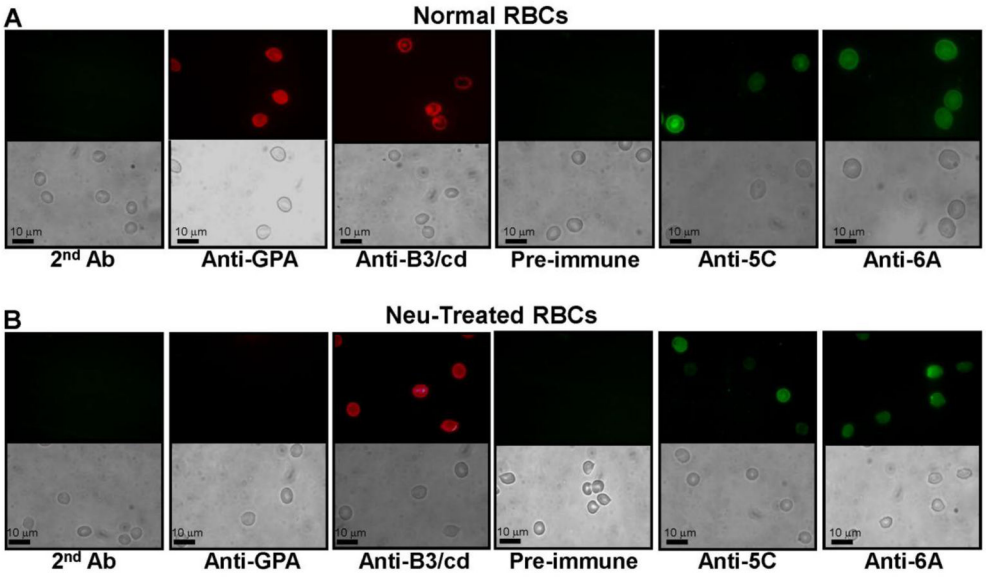

Fig. 2.

Reactivity of antibodies to fixed RBCs by indirect immunofluorescence assay. (A) Normal human RBCs reacting to anti-chicken secondary antibody (conjugated to Alexa 488), anti-GPA mAb against extracellular residues, anti-band 3 mAb against the cytoplasmic domain (anti-band 3/cd), preimmune IgY, mono-specific anti-5C IgY, and mono-specific anti-6A IgY are shown (100X magnification). Secondary antibodies were conjugated to either Alexa 488 or Alexa 594 to produce green or red fluorescence, respectively. Phase contrast is shown in the lower panel. (B) This panel shows reactivity to antibodies, as in panel A, in the neuraminidase-treated (Neu) RBCs.

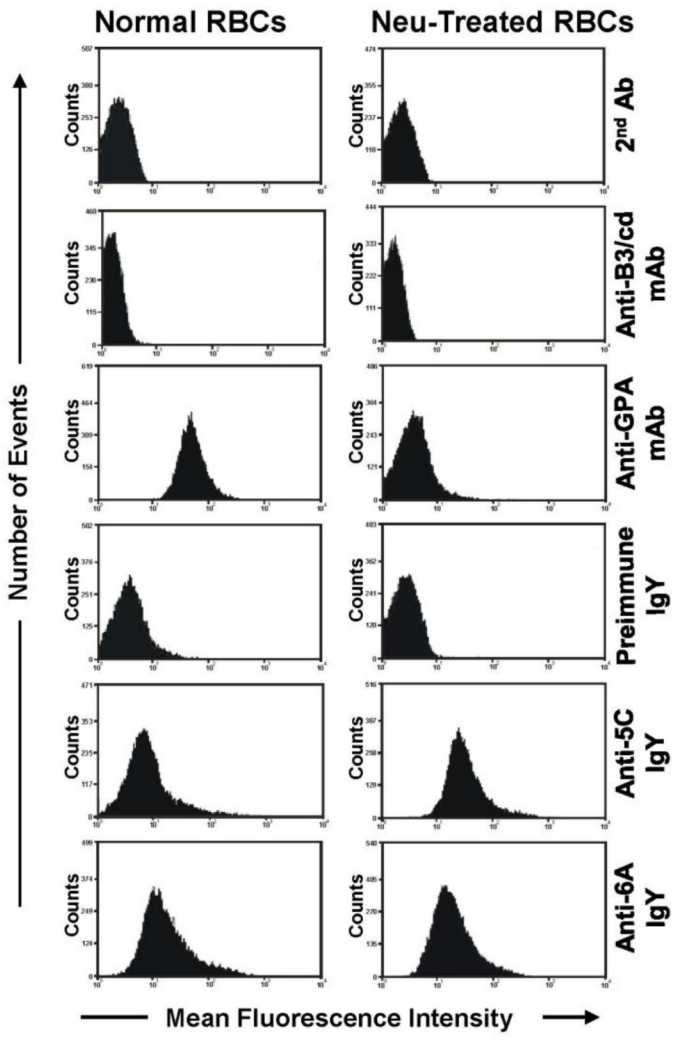

Fig. 3.

Binding of antibodies to intact RBCs by flow cytometry. Binding data obtained by flow cytometry were analyzed using histograms (x-axis, fluorescence intensity in logarithmic scale; y-axis, number of events) and then plotted on an identical x-axis (10^0 – 10^4 scale) for a visual comparison of fluorescence intensity. In both normal and Neu-treated RBC samples, binding measurements were performed with the following antibodies: anti-chicken secondary antibodies as controls, anti-band 3 mAb against the cytoplasmic domain (anti-band 3/cd), anti-GPA mAb against extracellular regions, and preimmune IgY. Fluorescence intensity for the binding of mono-specific anti-5C and anti-6A IgY antibodies (100 μg/ml) to RBCs was compared with the preimmune IgY (100 μg/ml) control.

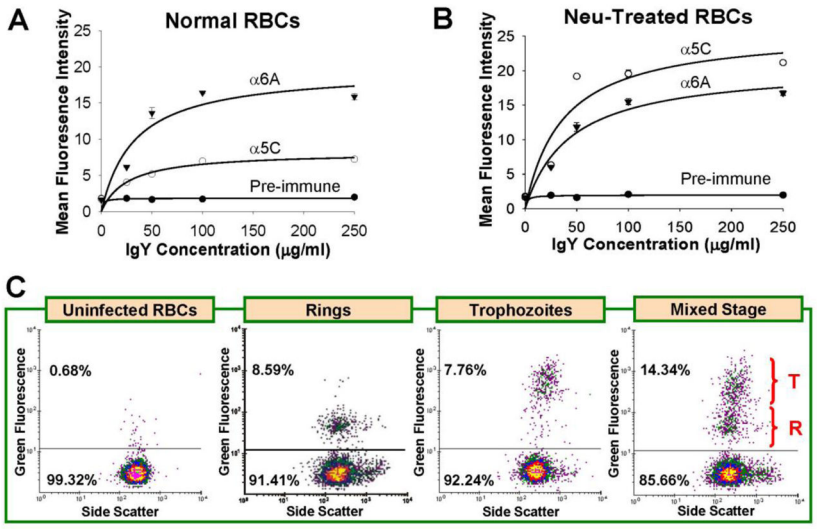

Fig. 4.

Binding of anti-band 3 IgY antibodies to human RBCs, and detection of parasitemia. (A) The concentration-dependent binding of anti-5C and anti-6A IgY antibodies (0, 25, 50, 100, 250 μg/ml) to human RBCs is shown. Mean fluorescence intensity (y-axis) was obtained from triplicate measurements using flow cytometry. The binding of preimmune IgY at all concentrations was insignificant. (B) Identical assay to (A) but with neuraminidase-treated RBCs. (C) Density plot analysis of parasitemia estimation by flow cytometry using SYTO-13. Culture of *P. falciparum* (3D7 strain) at a mixed stage was split into two samples. One sample was synchronized with sorbitol, while the other was kept as the mixed stage. When synchronized culture reached the trophozoite stage, both culture samples were fixed with 1% paraformaldehyde in PBS. An aliquot (25 μL) of the fixed sample was added to a 500 μL solution of SYTO-13 in PBS (final concentration 100 nM) and subjected to flow cytometry as described in Experimental Procedures. The density plot for each sample is shown with side scatter on the x-axis and FL2 (SYTO-13) on the y-axis, respectively, in logarithmic scale. While the mixed-stage sample (Infected/Unsync) contained young ring-stage parasites (R) as well as mature trophozoites (T), synchronized culture sample (Infected/Sync) showed predominantly trophozoites. Uninfected RBCs were used as control.

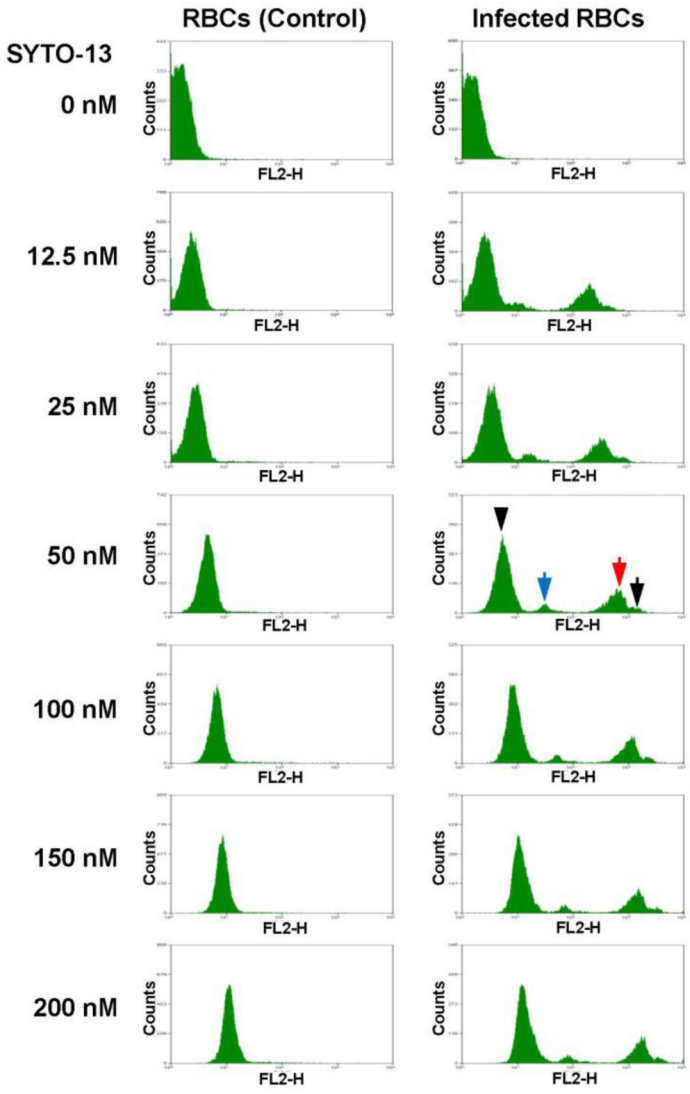

Fig. 5.

Histogram analysis of parasitemia by flow cytometry using SYTO-13. A mixed-stage *P. falciparum* culture was fixed as above and added to SYTO-13 solution to give a final concentration of SYTO-13 at 0, 12.5, 25, 50, 100, 150, and 200 nM in saline. Uninfected RBC samples were used as control. Flow cytometry data for infected and uninfected RBC samples were plotted as a histogram showing FL2 (SYTO-13) on the x-axis in logarithmic scale (10^0 – 10^4) and number of events on the y-axis. At 50 nM SYTO-13, uninfected RBCs (black arrowhead), ring-stage parasites (blue arrow), trophozoites (red arrow), and early schizonts (black arrow) had a clear baseline separation in the histogram. At 100 nM SYTO-13, there was a similar distinction of the cell populations but the background fluorescence was higher.

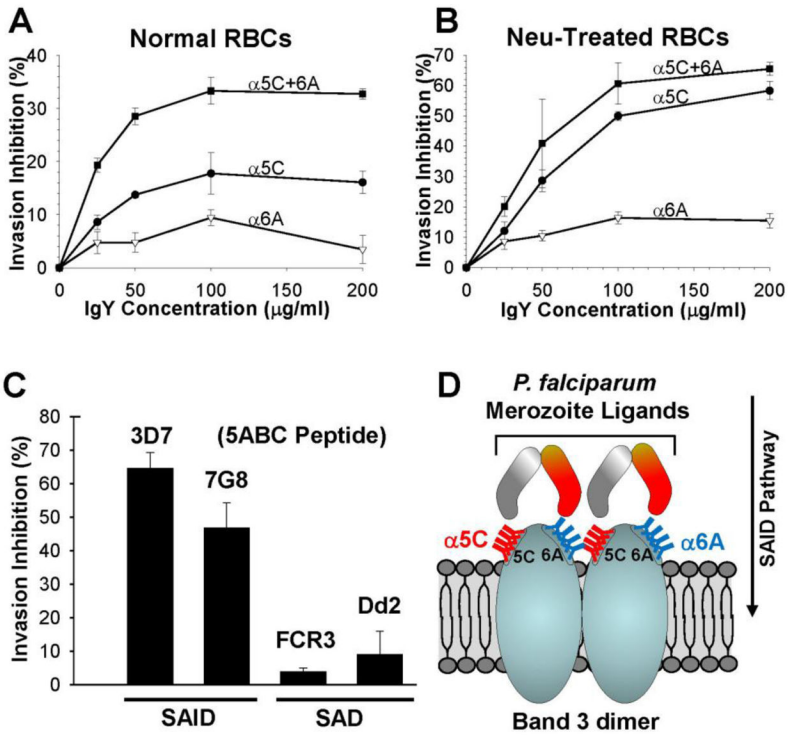

Fig. 6.

Antibody and peptide-dependent inhibition of *Plasmodium falciparum* invasion in RBCs. (A) RBC invasion assay was carried out using freshly added normal or (B) Neu-treated human RBCs in trophozoite-enriched *P. falciparum* (3D7 strain) samples having different concentrations of anti-band 3 IgY antibodies (see Experimental Procedures). Each anti-5C and anti-6A IgY was used at 0, 25, 50, 100, and 200 μg/ml concentrations either as a single inhibitor or as a mixture of the two. Newly formed ring-stage parasites were counted by the flow cytometry method using SYTO-13, and mean parasitemia (new infection) was determined from triplicate assay samples. The data are presented as percent invasion inhibition (mean ± s.e.) based on the preimmune IgY control sample taken as 0% inhibition (or 100% invasion). (C) Invasion inhibition assays were carried out for both SAID and SAD invasion phenotypes of *P. falciparum*. The assays were performed in triplicate using 8.0 μM of soluble recombinant proteins, GST-5ABC and GST (control). Student's *t*-test was used to compare the mean. The data presented as percent invasion inhibition is based on the GST control sample taken as 0% inhibition. (D) Illustration of the proposed model of the band 3-parasite interactions occurring at both 5C and 6A regions. Invasion is reduced when these interactions are inhibited through the use of recombinant peptides or antibodies against these regions.

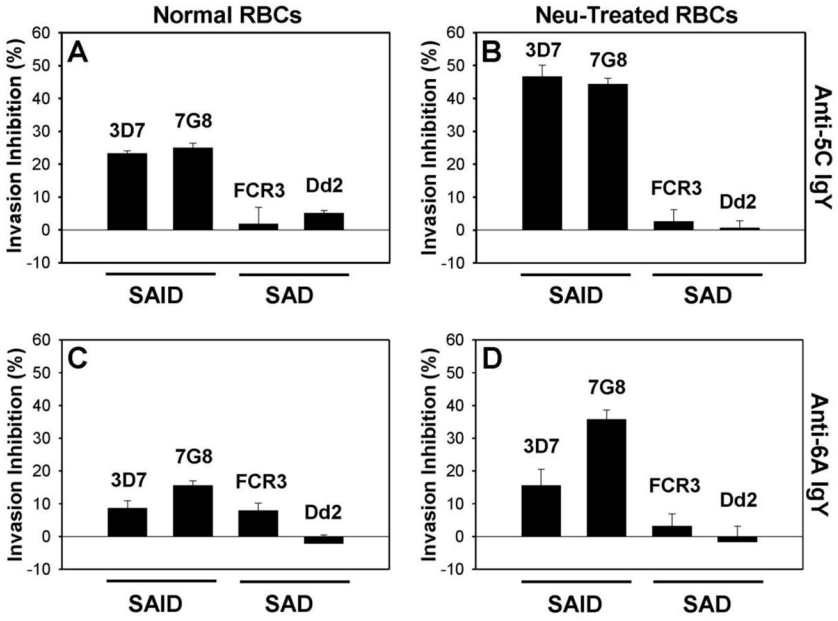

Fig. 7.

Invasion phenotype-specific inhibition of *P. falciparum* invasion into RBCs. (A–D) Using 100 μg/ml of anti-5C, anti-6A, and preimmune IgY as inhibitors, invasion inhibition assays were carried out for both SAID and SAD invasion phenotypes of *P. falciparum*. The assays were performed in triplicates using normal and Neu-treated RBCs. Flow cytometry using SYTO-13 allowed rapid analysis of multiple assay samples as described before. Results are presented as percent invasion inhibition (mean ± s.e.) where the preimmune IgY sample was taken as 0% inhibition. Student's *t*-test was used to compare the mean.

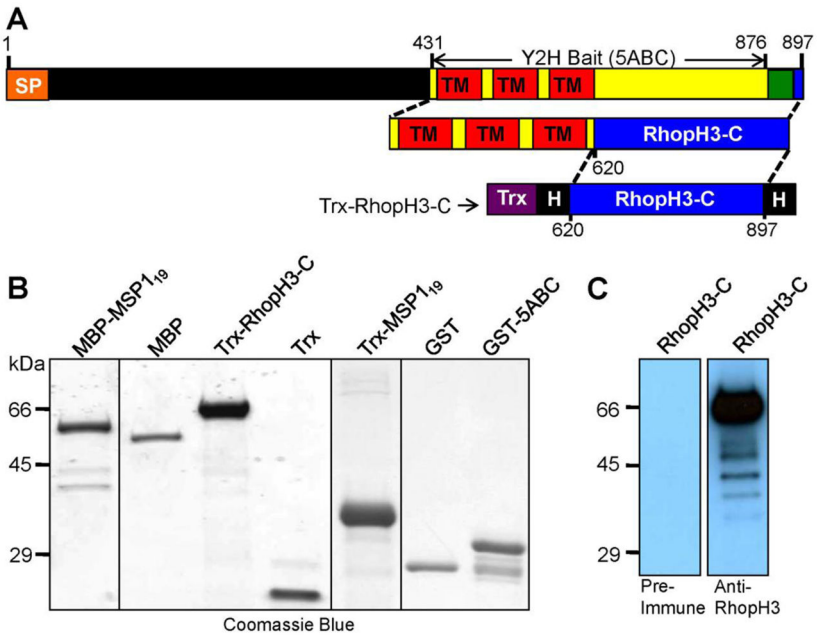

Fig. 8.

Identification Band 3-RhopH3 interaction by the yeast two-hybrid screen. (A) Diagram of full-length RhopH3 protein with its predicted transmembrane domains colored in red [47], the antibody epitope used in this study is shown in green, and the region identified as binding to the 5ABC domain of band 3 in a Y2H screen is colored in yellow marked with arrows. Recombinant RhopH3 was expressed by excluding the predicted transmembrane domains for optimum protein stability. This construct contains an N-terminal thioredoxin (Trx) tag, and both an N-terminal and C-terminal 6-His tag, and it was termed Trx-RhopH3-C. (B) Purified recombinant proteins include Trx-RhopH3-C, its band 3-binding site (GST-5ABC), Trx-MSP1$_{19}$, and respective fusion tags (MBP, Trx, GST). Gel was stained with Coomassie blue. (C) Polyclonal antibody was raised against the RhopH3 peptide (amino acids 876-892), and characterized by ELISA and Western blotting. This antibody was used to confirm the identify recombinant Trx-RhopH3-C by Western blotting.

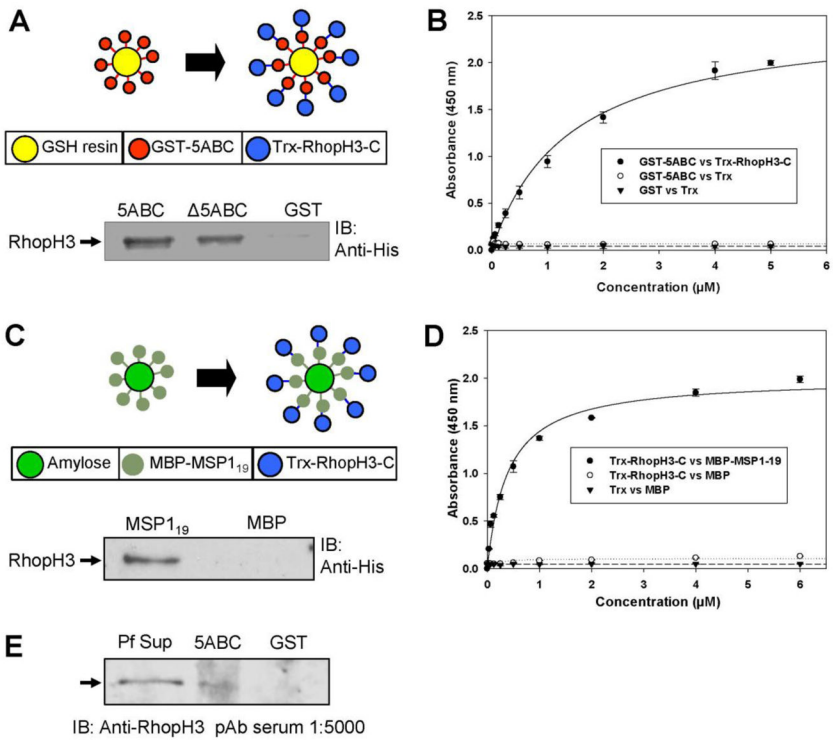

Fig. 9.

Biochemical interactions between RhopH3, Band 3, and MSP1. (A) The 5ABC region of band 3 was expressed as a GST fusion protein, which was then bound to GSH resin. Trx-RhopH3-C was added to the mixture and allowed to bind. After washing, bound protein was eluted and analyzed by immunoblotting against the His tag to detect RhopH3-C fusion protein. (B) Concentration-dependent binding of soluble Trx-RhopH3-C (0–5 μM) to GST-5ABC (0.1 μM) immobilized to an ELISA plate. The values are (means ± S.D.), and the dissociation constant was estimated from duplicate measurements. The ligand binding curves are shown in the range of 0–5 μM. Trx binding to GST-5ABC and GST was insignificant. (C) MSP1$_{19}$ expressed as MBP fusion protein was immobilized to amylose beads. Trx-RhopH3-C was added to the mixture, allowed to bind, washed, and eluted. Immunoblotting against the His tag was used to detect the RhopH3-C fusion protein. (D) Concentration-dependent binding of soluble MBP-MSP1$_{19}$ (0–6 μM) to Trx-RhopH3-C (0.1 μM) immobilized to an ELISA plate. The ligand binding curves are shown in the range of 0–6 μM. Trx-RhopH3 binding to MBP and Trx binding to MBP were insignificant. (E) Parasite culture supernatant was incubated with immobilized GST-5ABC protein, and binding was detected by immunoblotting using anti-RhopH3 serum. All pull-down binding assays were performed at least two times and some were repeated 4–5 times.

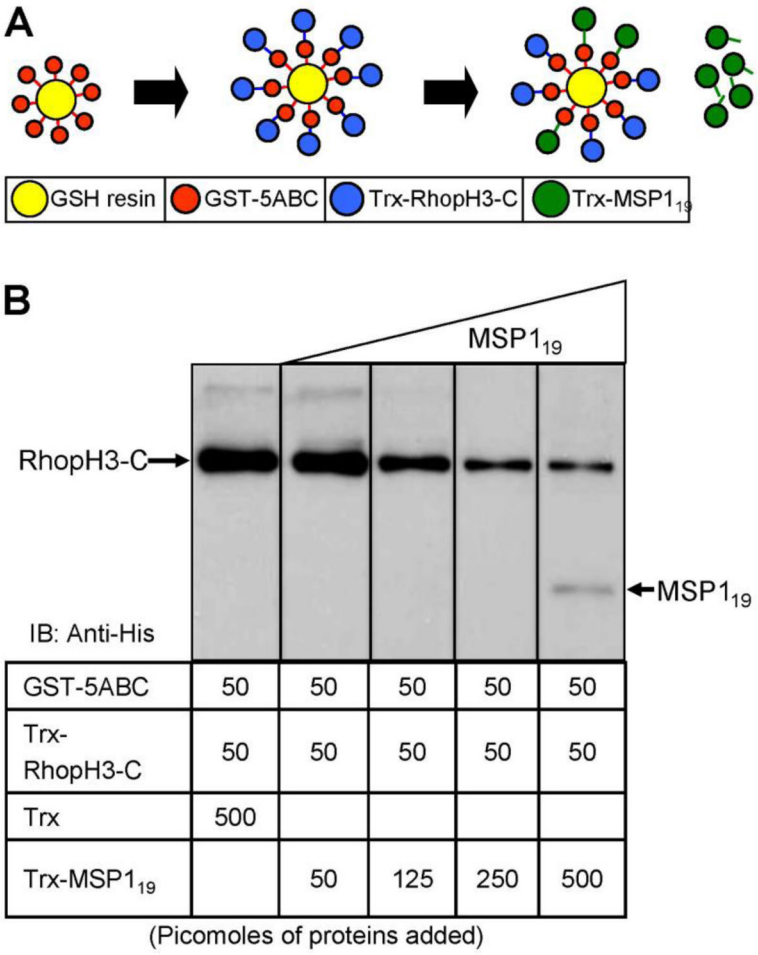

Fig. 10.

Competitive displacement of interactions between RhopH3, Band 3, and MSP1 binding domains. (A) 5ABC peptide of band 3 was expressed as GST fusion protein bound to GSH resin beads. Beads were allowed to interact with Trx-RhopH3-C, followed by the addition Trx-MSP1$_{19}$ at varying concentrations. (B) Bound proteins were eluted and analyzed by immunoblotting against the His tag to detect Trx-RhopH3-C and Trx-MSP1$_{19}$ fusion proteins. Trx-RhopH3-C was added to saturate the binding sites of GST-5ABC on beads. Increasing amounts of Trx-MSP1$_{19}$ were added to determine the displacement of RhopH3-C interaction with the GST-5ABC peptide immobilized onto beads.

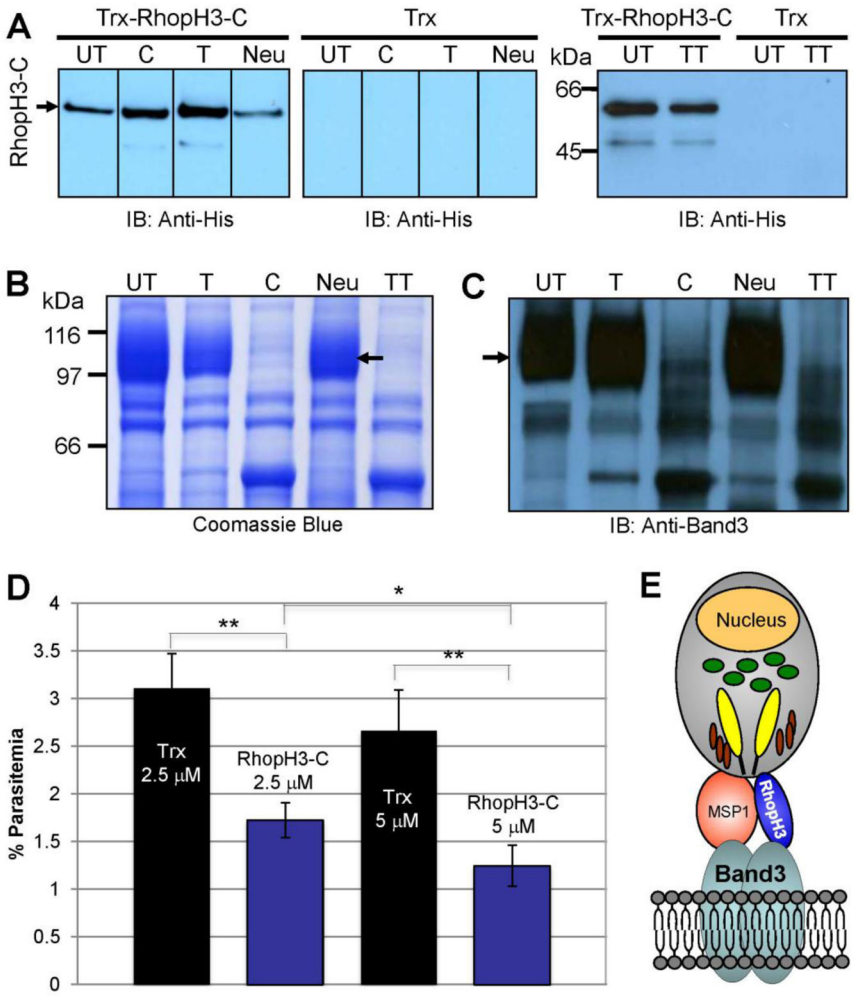

Fig. 11.

RhopH3 binds to RBCs and inhibits parasite invasion. (A) Untreated and enzyme-treated RBCs were incubated with Trx-RhopH3-C to allow binding. RBCs were washed and bound Trx-RhopH3-C was eluted with high NaCl. Eluted protein was analyzed by immunoblotting as described before. (B) Untreated and enzyme-treated human RBCs were used to prepare ghosts for analysis by SDS-PAGE and Coomassie blue staining. (C) Western blotting of the material shown in panel B using an anti-band 3 antibody. The arrow indicates the position of band 3 in untreated RBC ghosts. UT, untreated; C, chymotrypsin-treated; T, trypsin-treated; Neu, neuraminidase-treated; TT, Triple-treated C+T+Neu. (D) Invasion inhibition assay was carried out using the 3D7 strain of *P. falciparum*. The invasion assays were performed in triplicate at 2.5 and 5 μM concentrations due to the limitation of protein stability of recombinant Trx-RhopH3-C under these conditions. Trx protein was used as a negative control. (E) Proposed model of merozoite attachment to RBCs via interactions involving band 3, MSP1, and RhopH3.

Table 1

Equilibrium binding constants

	Bmax (mean fluorescence intensity)		Kd (μg/ml)	
Antibodies	**Normal RBCs**	**Neu-treated RBCs**	**Normal RBCs**	**Neu-treated RBCs**
Anti-5C IgY	8.2 ± 0.7	25.8 ± 2.7	25.7 ± 7.9	36.6 ± 12.5
Anti-6A IgY	19.6 ± 1.7	20.7 ± 1.4	32.7 ± 9.6	43.7 ± 8.9

Table 2

IgY concentration-dependent inhibition of RBC invasion by the *P. falciparum* 3D7 strain

		% Parasitemia (mean +/− s.e)				
		IgY concentration (μg/ml)				
RBCs	**IgY**	**0**	**25**	**50**	**100**	**200**
Normal	Pre-immune	3.19 +/− 0.03	2.99 +/− 0.14	3.01 +/− 0.11	3.00 +/− 0.02	2.98 +/− 0.11
	Anti-5C	---	2.31 +/− 0.04	1.97 +/− 0.02	1.89 +/− 0.03	1.78 +/− 0.02
	Anti-6A	---	2.61 +/− 0.03	2.21 +/− 0.04	2.16 +/− 0.13	2.11 +/− 0.01
	Both	---	1.37 +/− 0.04	1.16 +/− 0.01	1.00 +/− 0.12	1.04 +/− 0.02
Neu-treated	Pre-immune	1.39 +/− 0.01	1.35 +/− 0.07	1.29 +/− 0.06	1.30 +/− 0.03	1.41 +/− 0.01
	Anti-5C	---	0.97 +/− 0.11	0.67 +/− 0.03	0.58 +/− 0.01	0.53 +/− 0.01
	Anti-6A	---	1.11 +/− 0.01	0.98 +/− 0.01	0.87 +/− 0.02	0.81 +/− 0.07
	Both	---	0.44 +/− 0.03	0.21 +/− 0.01	0.16 +/− 0.05	0.17 +/− 0.02

Table 3

Inhibition of RBC invasion using 3D7, 7G8, FCR3, and Dd2 strains of *P. falciparum*

% Parasitemia (mean +/− s.e)*				
IgY Inhibitors				
Strains	**RBCs**	**Pre-immune**	**Anti-5C**	**Anti-6A**
3D7	Normal	3.63 +/− 0.03	1.73 +/− 0.07	2.63 +/− 0.03
	Neu-treated	0.97 +/− 0.18	0.57 +/− 0.01	0.86 +/− 0.05
7G8	Normal	2.69 +/− 0.07	1.56 +/− 0.03	2.18 +/− 0.04
	Neu-treated	1.02 +/− 0.06	0.39 +/− 0.01	0.75 +/− 0.02
FCR3	Normal	3.11 +/− 0.01	4.04 +/− 0.24	2.96 +/− 0.02
	Neu-treated	0.22 +/− 0.05	0.12 +/− 0.07	0.17+/− 0.03
Dd2	Normal	3.77 +/− 0.13	2.71 +/− 0.04	3.11 +/− 0.22
	Neu-treated	0.17 +/− 0.15	0.09 +/− 0.01	0.11+/− 0.01

* (Number of ring-infected RBCs after invasion/Total RBCs) × 100